Call: H2020-NMBP-2016-2017
Topic NMBP-06-2017
Research and Innovation Action

GRANT AGREEMENT NUMBER — 760824

RESHEALIENCE

Rethinking coastal defence and Green-energy Service infrastructures through enHancEd-durAbiLity high-performance cement-based materials

RESHEALIENCE
Ultra High Durability Concrete

D5.2 – Verification of sensitivity and reliability of non-destructive methods and sensors

Deliverable No.			5.2
Related WP			WP5
Related Task			5.2
Deliverable Title	Verification of sensitivity and reliability of non-destructive methods and sensors		
Deliverable Date			M22 (31 Oct 2019)
Deliverable Type			REPORT
Dissemination level			PU
Author(s)	**UPV**	Juan Soto, Manuel Valcuende, José Manuel Gandía, Ana Martínez	
	CSIC	Mª Cruz Alonso, María Criado, Mercedes Giménez	
	TUD	Christof Schröfl, Michaela Reichardt, Marko Butler, Viktor Mechtcherine	
	EGP	Francesco Animato, Sandra Scalari	
	BGU	Alva Peled, Oren Regev, Raghu Sripada	
	UoM	Ruben Paul Borg	
Checked by	Juan Soto/Manuel Valcuende/José M. Gandía/ Mª Cruz Alonso		
Reviewed by (if applicable)	Maria Cruz Alonso and Liberato Ferrara		
Approved by	Liberato Ferrara		
Status	Final		

Disclaimer/ Acknowledgment

This project has received funding from the European Union's Horizon 2020 research and innovation programme under grant agreement No 760824. The information and views set out in this publication does not necessarily reflect the official opinion of the European Commission. Neither the European Union institutions and bodies nor any person acting on their behalf, may be held responsible for the use which may be made of the information contained therein.

Publishable summary

The document aims to verify the sensitivity and reliability of non-destructive techniques (NDT) and sensors which can be used for durability monitoring of Ultra-High Durability Concrete (UHDC) structures. The high compactness of UHDCs, their high content of anhydrous cement particles or their high content of steel fibres, very often added to the mix composition, could affect the measurement or even the applicability of some NDTs. Therefore, it is important to ensure that these techniques, whose measurements provide the basis for durability design models in conventional concrete (CC) constructions, are also valid for UHDC constructions.

According to the damages that may happen in (marine) XS and (Industrial) XA environments, different NDTs have been evaluated and the results have been analyzed providing information about the most suitable measurement systems to obtain durability parameters in situ. This document will serve as a basis to select the most suitable in-situ NDT systems to be employed in pilot-scale validation located in XS and XA environments.

In the first part of the Deliverable, the durability parameters based on NDT have been grouped in different categories and different techniques have been described briefly, also indicating whether they are applicable in laboratory or on-site:

1) Mechanical parameters of concrete: Ultrasonic Pulse Velocity, Acoustic Emission, Sclerometric Index and Strain.
2) Physical parameters of concrete: Gas Permeability, Water Permeability, Electrical Resistivity, Moisture and Temperature.
3) Chemical parameters of concrete: Chlorides, pH, and Aggressive Ion Detection.
4) Electrochemical parameters of reinforcement: Corrosion potential and Corrosion rate
5) Mechanical parameters of reinforcement: Rebar deformation

Factors that may affect the reliability of measurements have been analyzed and results from lab tests performed on UHDCs are presented. Moreover, the sensitivity has been assessed in order to verify if these techniques are able to differentiate processes such as ageing, the presence of aggressive ions or cracks, among others.

The results have demonstrated that some standard procedures or techniques are suitable for UHDCs. In other cases, it is necessary to establish specific protocols and some NDTs are not recommended because of their low sensitivity.

Table of contents

List of acronyms, abbreviations and definitions

AE	Acoustic Emission
ANF	Alumina NanoFibers
CA	Crystalline Additive
CC	Conventional Concrete
CN	Both types of Nano-Cellulose
CNC	Cellulose NanoCrystals
CNF	Cellulose NanoFibrils
FBG	Fibre Bragg Grating
HPC	High-Performance Concrete
i_{CORR}	Corrosion current density
LVDT	Linear Variable Differential Transformer
R_p	Polarization resistance
RE	Reference Electrode
SCE	Standard Calomel Electrode
TRC	Textile Reinforced Concrete
UHDC	Ultra-High Durability Concrete
UHPC	Ultra-High Performance Concrete
UPV	Ultrasonic Pulse Velocity
v_{CORR}	Corrosion rate

Index of tables

Index of figures

1. Scope of the document

Deliverable 5.2 focuses on non-destructive monitoring tests. Several parameters related to the material durability in conventional concretes (CC) are usually determined with non-destructive measurement techniques. The reliability of these techniques may be questionable in Ultra-High Durability Concretes (UHDCs) because of the high compactness of their matrix and the high content of steel fibres. Therefore, it is important to ensure that these techniques, on whose measurements of the durability design models are based in CC constructions, are also valid for UHDC constructions.

In the first part of the document (section 2), a review of the NDT and sensors that can be employed for monitoring the most representative durability parameters is done. This review has been carried out considering the expected damages for reinforced concrete structures exposed to XS and XA environments, which have been identified in D3.1 and D3.2. Afterwards, in the second part of the document (section 3), the applicability of some of these methods to UHDCs has been investigated, analyzing their sensitivity and reliability when used in structural elements made with this type of concrete. The obtained information will serve as a basis to select the most suitable in-situ NDT systems to be employed in pilot-scale validation.

- ***Durability parameters to assess by NDT methods in XS environment***

According to pathology studies reported in D3.1 and D3.2, derived from pilot partners experience, typical damages in structures under marine exposure conditions, XS environment, mainly consist of excessive and premature corrosion of reinforcement, due to the penetration of chlorides inside the concrete. Once the chloride ions have reached the reinforcing bar and destroyed the passivating layer, the kinetics of the corrosion processes depends on the presence of oxygen and moisture according to the characteristics of the concrete designed. In this sense, the parameters to be monitored in this environment are essentially the identification of the chloride transport and the detection of the reinforcement corrosion onset.

The use of textile reinforced concrete in the XS environments eliminates the damage as consequence of corrosion of reinforcements but concrete deformation and concrete cracking along time are of great monitoring interest, since the tightness of the structural body against ingress of water is essential to ensure durability.

- ***Durability parameters to asses by non-destructive methods in XA environment***

According to pathology studies reported in D3.2, the damage in structures under XA environment includes the concrete cracking due to expansion, in the case of sulphate attack, and the dissolution of the cement paste, in the case of acid environments. In reinforced concrete structures exposed to these aggressive environments also corrosion of reinforcements is expected, mainly driven by chlorides and neutralization of concrete by interaction with CO_2 waters. Carbonation and corrosion of concrete by industrials fluids containing carbon dioxide are quicker than in air, due to the acidification, which may lead to severe degradation within just a few months.

Although the control of degradation processes under XA environment is usually more complex, the durability related parameters that can be monitored with sensors or NDT methods are: concrete cracking, aggressive penetration, such as chloride ions, or pH decrease, and volume deformations together with parameters dealing with reinforcement corrosion onset.

2. Durability parameters based on non-destructive techniques (NDT)

By means of Non-Destructive Techniques (NDT) or sensors, several parameters related to reinforced concrete durability can be determined. Table 1 shows the NDT being described in this section.

Table 1. NDT related to reinforced concrete durability.

Material	Parameter/Property	NDT
Concrete	Mechanical parameter	- Ultrasonic pulse velocity (CSIC, UPV) - Accoustic emission (BGU) - Sclerometric index (EGP) - Deformation (TUD)
	Physical properties	- Gas permeability (UPV) - Water permeability (TUD, UOM) - Electrical resistivity (CSIC, UPV) - Moisture (UOM) - Temperature (UOM, UPV)
	Chemical parameters	- Chlorides (UPV) - pH (TUD, UOM, UPV) - Aggressive ions (CSIC, UPV)
Rebar	Corrosion risk	- Corrosion potential (UPV, CSIC) - Corrosion rate (UPV, CSIC)
	Mechanical parameter	- Deformation (UPV)

2.1. NDT to measure mechanical parameters of concrete

2.1.1. Ultrasonic Pulse Velocity (UPV)

The UPV method is based on the velocity of the propagation of ultrasonic waves in hardened concrete to determine concrete quality and defects as cracks. The measurement of the velocity of ultrasonic pulses of longitudinal vibrations may be used for the following purposes:

- determination of the homogeneity of concrete in and between structural members
- measurement of changes occurring with time in the properties of concrete
- correlation between pulse velocity and strength as a measure of concrete quality.
- determination of the modulus of elasticity and dynamic Poisson's ratio of concrete.

The wave velocity depends on the elastic properties and density of the concrete. The response of a heterogeneous elastic body to a propagating wave is a function of the wavelength in comparison with the length scale of the heterogeneities. This technique is strongly influenced by the size and distribution of the heterogeneities in the concrete and the wavelength (and therefore frequency) of the wave field.

The transmitting transducer of the pulse velocity instrument propagates the ultrasonic wave into the concrete and the transducer receives the pulse pass through the concrete at another point. The pulse velocity instrument display indicates the transit time; i.e. the time it takes the compressional wave pulse to travel through the concrete. The propagation velocity is calculated as the ratio between the distance between transducers and the transit time (Figure 1).

To transmit or receive the pulse, the transducers must be in full contact with the test sample; otherwise, an air pocket between this and transducer may introduce an error in the indicated transit time. This error is introduced because only a negligible amount of wave energy can be transmitted through the air. To overcome this drawback couplant are used, typicall including high conductive gels as petroleum jelly, grease, soft soap, gel, and kaolin/glycerol paste.

There are three possible configurations in which the transducers may be arranged, as shown in Figure 1. These are direct transmission (opposite faces); semidirect transmission (adjacent faces); and indirect or surface transmission (the same face).

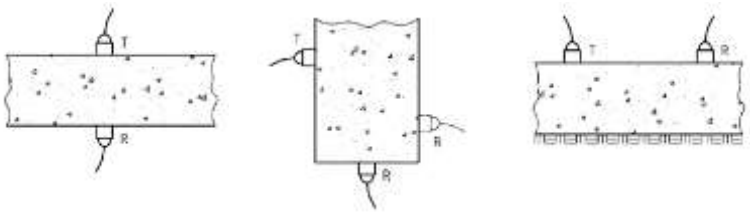

a) b) c)

Figure 1. Pulse velocity measurement configurations. a) Direct method; b) Semidirect method; c) Indirect method [EN 12504-4]

2.1.2. Acoustic emission

Acoustic Emission (AE) system is a non-destructive technique widely used for monitoring concrete structures. Any deformation in the concrete (or cementitious) matrix is accompanied by elastic waves, which can travel through the matrix medium. Detecting these elastic waves can provide crucial information about the health of the structures, failure mechanisms, crack propagation and corrosion. The elastic waves generated in the concrete structures are detected by AE sensors (piezoelectric transducers). These sensors transform the elastic waves into electrical waves, which are further recorded by a computer or data acquisition system. AE parameters, such as amplitude, absolute energy, cumulative absolute energy, rise angle and average frequency, allow to characterize the cracked state of the material.

The test is carried out placing several acoustic emission sensors along the specimen length. Deformation or a crack produced in the specimen under load becomes a source of a mechanical wave which is recorded by the AE sensors. Absolute energy of such detected waves provides a measure of how intense the crack is.

2.1.3. Sclerometric index

Sclerometer test is aimed at estimating the concrete strength by measuring the surface hardness; the latter being assessed by evaluating the rebound of a metal sphere contained in a special hollow cylinder. The sclerometer consists of a spring that pushes a percussion rod which is in direct contact with a concrete surface. The mass is charged by the

spring with a constant amount of energy and then it is released in order to strike against the concrete surface. The instrument allows measuring the rebound index of the aforementioned mass, which, on equal terms of the instrument (springs, frictions, weight of the mass), depends exclusively on the physical and mechanical characteristics of the material under examination.

As indicated by the related standard (EN 12504-2:2012. Testing concrete in structures. Non-destructive testing. Determination of rebound number), the rebound index must be evaluated as the average of a prescribed number of beatings performed in the same area whose surface has been properly prepared in order to be free of roughness. The test is able to provide the following information:

- curing of the concrete;
- a rough estimate of concrete mechanical strength, by measuring the surface hardness.

The test is performed by placing the sclerometer in contact with the surface of the concrete structure to be monitored and perpendicularly to it, after treatment with a medium-grain abrasive stone in carborundum, and measuring the rebounds of a steel cursor pushed hard on the surface. The test result is given in terms of average rebound index **Ir** and is reported for each investigated point. The presence of highly carbonated concretes can affect the measures of surface hardness.

2.1.4. Concrete deformation

Strain-gauges based on electrical resistivity change

Typical strain-gauges consist of thin plastic sheets with resistance wire and electrical connectors. They are attached with a suitable adhesive to a specific point on the structural element, which is then mechanically loaded and deforms. The deformation is transferred to the strain gauge and leads to changes in electrical resistance due to change in length and cross-section. Stretching of the strain gauge leads to increased electrical resistance, compression to decreased resistance. From the measured changes in electrical resistance and the known material properties of the strain gauge, the strain is calculated. The range of strain gauge products is wide and there are general as well as specified solutions considering the ranges of application. Several metal and semiconductor materials are suited for the application in strain gauges. Different carrier films and adhesives are used to fix the strain gauge. The chosen materials determine:

- maximum strain,
- sensitivity of the strain gauge (describes the proportionality of resistance change to the strain = k-factor),
- measuring rate,
- temperature sensitivity,
- moisture sensitivity,
- creep behavior and, as a related long-term or durability issue, the drift of measurement values in time.

Depending on their geometry strain-gauges can be applied as linear sensors with a single measurement grid in one direction up to multiple measurement grids arranged as chains to measure strain courses or multiple grids in multiple directions, so-called rosettes.

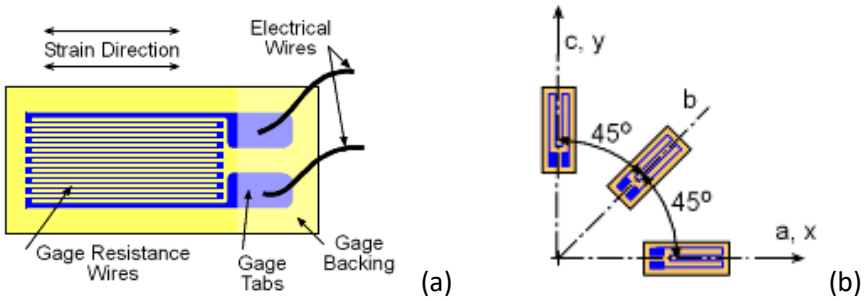

Figure 2. a) Strain-gauge; b) Strain-gauge Rosette at 45˚.

Fibre Bragg grating (FBG)

Light is sent through an optical fibre, which contains a core with a Bragg grating acting like a wavelength filter. A laser beam is used to generate a repeating microstructure, a permanent change in the physical properties of the glass matrix. When light is introduced into the optical fibre, light of a specific wavelength is reflected by the Bragg grating and determined. The rest of the light is transmitted. Due to temperature and strain variations of the grating the reflected wavelength changes. Considering the shift of the wavelength, the strain is calculated. Fibre Bragg grating lengths vary from a couple of µm to several mm and multiple gratings can be monitored in series. The sensor can be used to measure localized strain developments. They can be read out over large distances without the need for amplification. To suppress the cross-sensitivity between temperature and strain, a second sensor near the measuring point is set up separately to measure the temperature.

Linear variable differential transformer (LVDT)

A linear change in length is measured between a reference point and the position of the tip of the LVDT. The measurement principle is based on the development of a voltage in the secondary coils due to an unequal magnetic coupling by the linear movement of a soft iron core. The measured voltage is then correlated to the change in length (displacement) over the measurement base. If the measurement of a strain, rather than of displacement, is of interest, it can be calculated by relating displacement to the reference length. Depending on the application the sensor measuring range can be chosen from 1 mm to several hundreds of mm. The LVDT is positioned on the external surface of a structural element. It can be fixed to the structures by means of screwed or glued supports.

Photogrammetric method

Length change of reinforced concrete and formation of the characteristic multiple crack pattern upon mechanical tensile loading can be detected by photogrammetric methods in laboratory setup. A black and white arbitrary speckle pattern is paint brushed to the specimen surface. Photo sequences are taken during the loading experiment, whereby the camera is fixed at a pre-defined position. Digital Image Correlation (DIC) procedures and algorithms visualize length change and, most importantly, crack formation from the micrometer range onwards. Such technique could be most valuable for monitoring a real-scale structural unit made of UHDC. However, it has been demonstrated neither on the fundamental-scientific nor the application-oriented levels. The boundary conditions of the ReSHEALience project do not allow for implementing this method to the UHDC demonstrator structures, because the risk of fundamental failure is too high. Most critical issues with respect to the method are:

- Long-term visibility of the speckle pattern upon exposure to a natural environment at all;

- Ditto in the specific surrounding of a structure in XA environment (sea water, under water and splash zones, growth of algae or mussels, bleaching);
- Long-term maintenance of the fixed camera position with the level of precision that is required to detect meaningful changes in the speckle pattern;
- Durability of a camera system.

Embedded decoupled measurement bar

Deformation of structural elements can also be measured using a bar embedded in the concrete. On the one-meter-range, length changes and potential multiple crack formation should be assessed as an integral value. The occurrence of distinct crack positions is hard to predict. Figure 3 sketches the experimental setup.

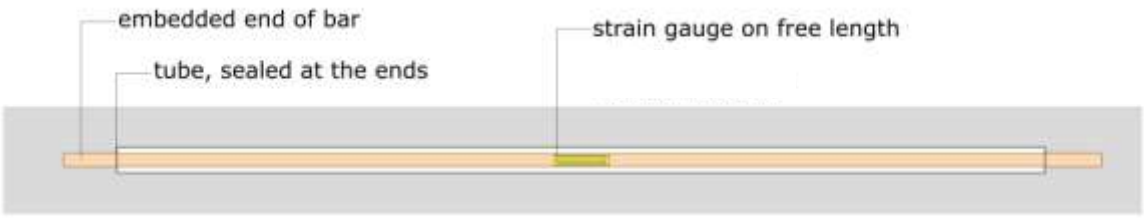

Figure 3. Embedded decoupled measurement bar for monitoring length change in TR concrete; bar length in the order of magnitude of one meter

A strain gauge is maturely and durably glued to a bar or wire, whereby the sensor itself may classically be based on resistivity or inductive principle. The sensor, its connecting electrical wires and the bar itself are encapsulated in a tube. The length of this tube is the measurement length inside the structural element because the bar can move smoothly inside the tube. The two ends of the bar, however, directly contact the concrete matrix (embedment during concrete casting). Hence, the tube length represents a mechanical decoupled area and allows for the detection of length changes, whereas its ends are load-carrying connections that have to move with the UHDC matrix. Data acquisition and evaluation are fully equivalent to any ordinary procedure related to the sensor itself.

2.2. NDT to measure physical properties of concrete

2.2.1. Gas permeability

The objective of this method is to study the ease with which a gas can penetrate in hardened concrete. The parameter that is determined during the test is the coefficient of gas permeability, K.

This coefficient is an indirect indicator of durability since it provides information on the material porosity. In some cases, the initiation and the rate of the rebar corrosion processes have been associated with gas penetration, such as O_2 and CO_2, into the concrete. Thus, some standards, such as the French PR NF P18-470, require this verification parameter for durability.

The test consists of applying oxygen under pressure on one of the faces of the specimen and measuring the flow of gas passing through the concrete section. During the test, by means of a vacuum pump, a vacuum is created in a test chamber and in a concentric guard-ring, both of which are open to the concrete surface. Then, the connection between the test chamber and the vacuum pump is air-tightly closed. The pressure rise in the test chamber, due to the air

flowing through the concrete, is measured as a function of time. The air permeability is computed as a function of the change in pressure with time and other characteristic values.

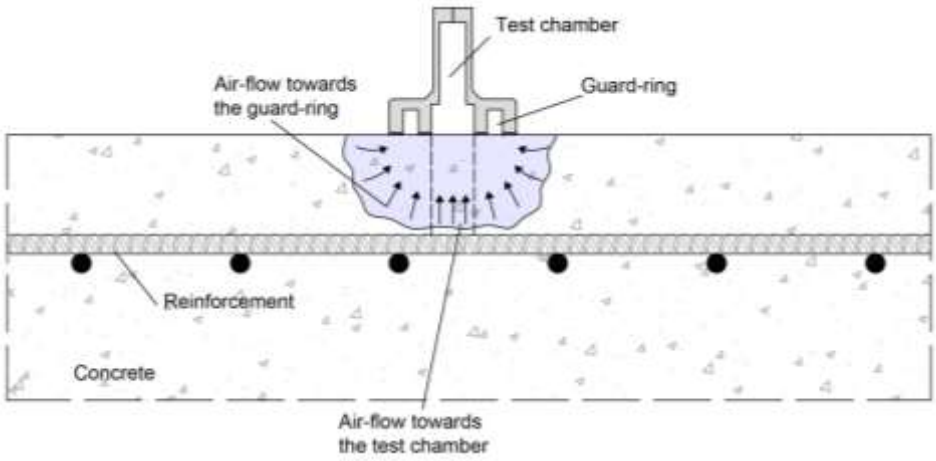

Figure 4. Air flow during the on-site test of the air permeability [SIA 262/1, 2013].

Air permeability can be measured in the laboratory on specimens or on concrete cores extracted from real structures. There is also the possibility of measuring the permeability on-site without the need to drill concrete cores, using commercial measurement equipment. The parameter obtained with the test is also a permeability coefficient. This method has been included in the Swiss standard SIA 262/1: 2013 as a standardized method.

2.2.2. Water permeability

There are various non-destructive techniques to evaluate water permeability, such as Karsten-tube, Pleyers-tube, Franke-plate, Figg test or Germann water permeation test.

Karsten-tube", "Pleyers-tube" or "Franke-plate

Capillary water penetration can be measured with Karsten-tube, Pleyers-tube or Franke-plate (Figure 5). All three setups enable a non-destructive measurement of water absorption by the surface. A glass tube with some water carrying volume is reversibly glued to the testing surface using a sealing compound. The volume and tube are filled with water and over time, the uptake through the testing surface is measured by reading the reduction of the water column in the tube. Afterward, the amount of water uptake is used to calculate the water absorption coefficient.

The boundary effect of the distribution of water in three dimensions is compensated by different ways in each method. The Franke-plate considers a comparatively big surface leading to a negligible boundary effect, while for the Karsten-tube two mathematical approaches are available to correct the results. The Pleyers-tube uses a secondary chamber which prevents a lateral transport of the water (Figure 6). Therefore, a correction is not necessary.

Figure 5. Franke-plate, Karsten-tube, Pleyers-tube [Haindl et al., 2016].

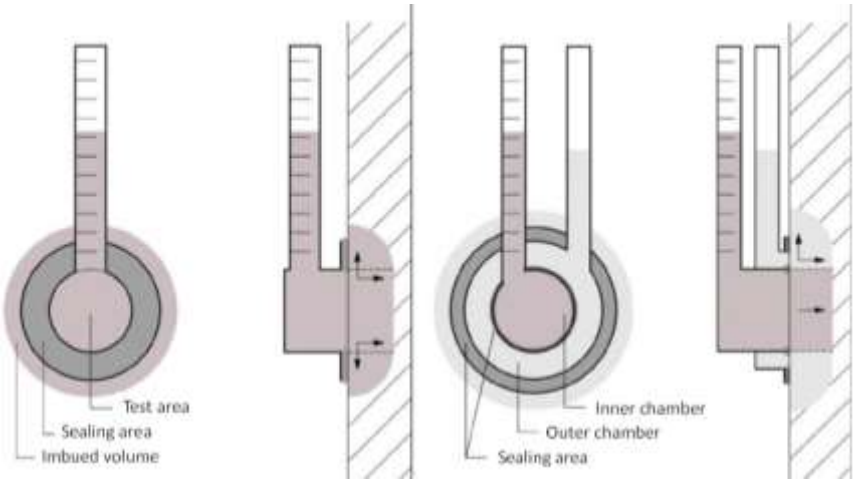

Figure 6. Schematic view of Karsten-tube (left) and Pleyers-tube (right) [Haindl et al., 2016].

All methods are sensitive to the conditions of the surface of the structural element. To ease the comparability of readings, afternoon measurements on a dried surface, several days after the last rainfall event are recommended. The applied amount of water in the tube reflects the wind forces and should be considered. Furthermore, the thickness of the sealing material may also affect the measured results. Therefore, several measurements should be taken and compared to results from laboratory tests.

The Figg test

This test measures water permeability by drilling a 5.5 mm diameter hole for 30 mm into the concrete element under investigation. A silicone sealant is placed on the top of the hole whilst a needle is inserted into the hole through the plug. A syringe is used to insert water into the drill hole. The water then flows back up the outer needle and into a horizontal length of the capillary tube. This tube is placed at a level of 100 mm above the bottom of the drill hole. During this test, the valve is closed and the time taken for the water to travel 50 mm is recorded.

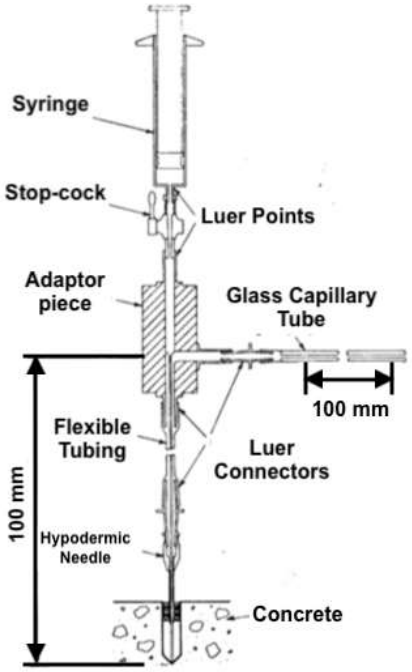

Figure 7. Apparatus for the Figg test [The Concrete Society, n.d.].

Germann water permeation test

The GWT (Germann Water Permeation Test) is an on-site non-destructive test which measures the permeability of the water into the concrete under an applied pressure. A pressure chamber that contains a watertight gasket is tightly secured to the surface by either a suction plate or by two anchored clamping pliers. The gasket can also be bonded to the surface with an adhesive instead. The chamber is then filled with water and the concrete surface is allowed to absorb the water for 10 minutes. The valve is closed whilst the top cap of the chamber is rotated until the selected water pressure can be seen on the gauge. As the water is permeating the concrete, the desired pressure is then maintained using a micrometer gauge which pushes a piston into the chamber. The time and the speed it takes for the piston to move is recorded in µm/s. This is then used to calculate how water permeable the concrete surface is [Germann, 2014].

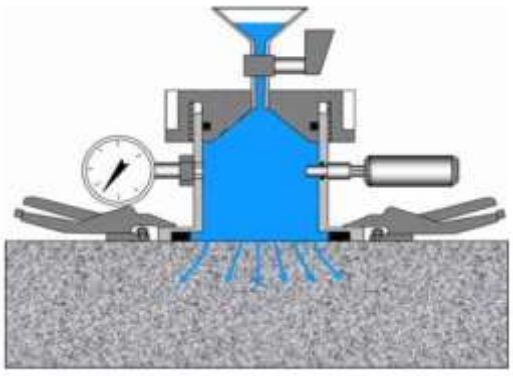

Figure 8. Germann water permeation test [Germann, n.d.].

2.2.3. Electrical resistivity

Electrical resistivity is a property that expresses the capacity of a material to transport electric charge. In concrete, electrical charges are mainly transported by ions dissolved in the pore solution, so it is possible to assume that aggregates act as electrical insulators because their resistivity is several orders of magnitude higher than that of the aqueous pore solution. Therefore, the electrical resistivity provides indications on the pore connectivity and, as a consequence, it is a parameter which is related to ions transport inside the concrete matrix and in some cases has been related to the corrosion risk of the reinforcement.

This method does not provide any quantitative information on the corrosion but offers an idea of the concrete changes during exposure to aggressive environments.

The laboratory reference method to measure the resistivity of a material is the direct method. It consists of applying a uniform electrical field with a resistivimeter. This electric field is applied between two electrodes in contact with the bases of the specimen (Figure 9). Specimens should not have metallic reinforcements inside their matrix, because they conduct current faster than concrete and, therefore, they disturb the current flow. Electrodes can be dense meshes or plates made of steel, copper or any other good metallic conductor of the same dimensions as the transversal section of the specimen. To ensure good electrical contact between the specimens and the electrodes, wet sponges of the same dimensions as the electrodes must be used.

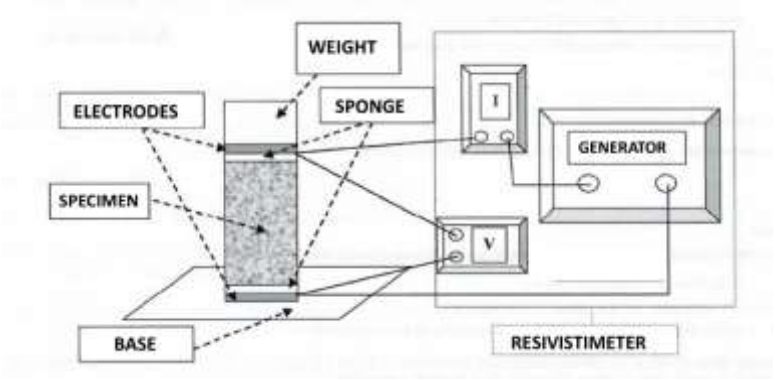

Figure 9. Set up of resistivity measurement by the direct method [UNE 83988-1, 2008].

In real concrete structures, this direct method is not applicable unless core specimens are extracted from the area under study, which then converts the test into a (semi)-destructive one. The reason is that, usually, the surface of the electrodes is smaller than the section of the area under study and because of the presence of rebars.

The resistivity of the surface concrete of a given structure can be measured non-destructively using electrodes placed on the concrete surface. The devices usually used for these measurements are based on the Wenner method (also known as four points method). As for the direct method, for its correct application, the concrete samples should not have metallic reinforcements in the measuring area. According to some research works, while measuring with four electrodes over bars at depths of 10 or 20 mm, errors can be made by a factor of 2 to 6. This method consists in the application of an electrical current between two electrodes placed on the concrete surface and then the measurement of the voltage between two other electrodes aligned within the two former ones and placed at a fixed distance (Figure 10, left). The ratio of voltage to current is resistance.

The measurement procedure consists in locating the reinforcement first with a pachometer and afterward performing the electrode measurements as far from the rebars as possible diagonally inside the rebar mesh (Figure 10, right). Five readings from the same area must be carried out, taking the median of the five values obtained as the result.

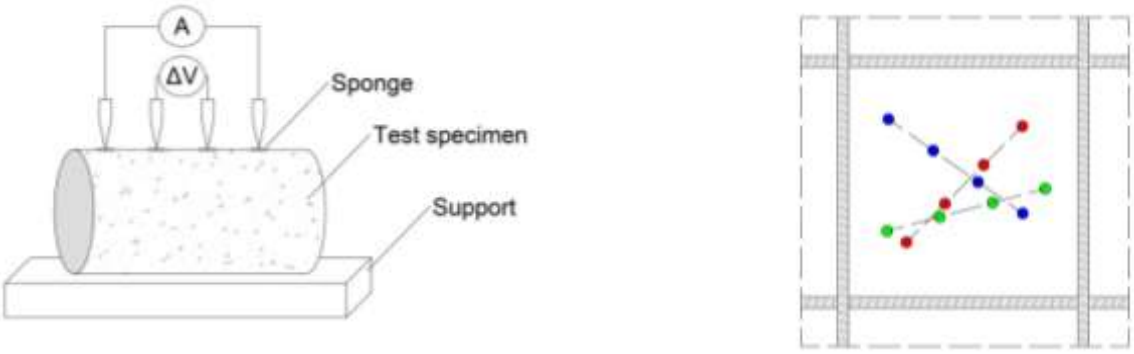

Figure 10. Left) Set up of four-electrode measurements. Right) Measurement inside the rebar mesh to minimize the influence of rebars.

Finally, it is important to mention that if the measurement of resistivity is planned for monitoring purposes, metal electrodes (usual pairs of small bars) may be installed before casting.

2.2.4. Moisture and temperature

Moisture

Moisture content in concrete may be measured through resistivity sensors, such as those illustrated in Figure 11**Errore. L'origine riferimento non è stata trovata.**. This type of setup is done by extracting a core from an existing structure and embedding pairs of graphite rods at different levels. The prepared core is reintroduced back in the structure and sealed with resin. A data acquisition system measures the changes in resistance which indicate the presence, or absence, of moisture. In the case of new structures, the rods may be prepared before hand and installed by securely connecting them to the mesh reinforcement before pouring of concrete. Since these sensors are passive, they do not require any battery power, thus making them useful for long-term monitoring.

Figure 11. Graphite rods embedded in a concrete core at different levels.

Temperature

There are several methods to measure the temperature, with various commercially available devices. The main two types are resistance temperature detectors (RTDs), and thermocouples. While both types are passive, the former method is more suitable for long-term readings. The basic concept of RTDs is based on the variation in resistance of a material with temperature, governed by equation 1. A typical commercial solution is the PT100 platinum sensor, having a reference resistance (R_{REF}) of 100 Ω at a reference temperature of 0° C. The temperature coefficient, α, is given as 0.00392. By reading the resistance of the solution, the temperature can be calculated.

$$R = R_{REF}[1 + \alpha(T - T_{REF})] \quad \text{eq. (1)}$$

Another method for reading temperature is by using thermocouples. Such devices consist of two different electrical conductors, which form a junction. The basic construction of a thermocouple is illustrated in Figure 12. The junction end, having a temperature T_2, is embedded in concrete while a voltmeter is connected to the tail end, with a temperature reference T_1. Since there is a temperature difference between the two ends, a potential difference can be measured using a data acquisition system.

Figure 12. Schematic of a thermocouple [Scerivini, 2009].

Other commercial solutions exist for reading temperature in concrete; however these tend to be based on active components with wireless communication. While these products are relatively simpler to install, their effective lifetime is limited as typical battery-operated sensors only last for a couple of months.

Temperature can also be measured with a thermographic camera. The camera does not measure temperature but registers the outcoming radiation from a body. Generally cameras work with long-wave infrared light (λ=8 to 12µm) which in general terms provides a stable spectrum, although some may work with shorter waves (λ=5 to 8µm).

The outcoming radiation of a body is formed by the reflected and the emitted radiations, and only the emitted radiation is associated with temperature. Thus, in order to know the real superficial temperature of a body by thermography a series of corrections on the received signal has to be performed, so that the temperature can be obtained from the radiation captured by the camera. Otherwise, the data in the image would correspond to an apparent temperature.

This correction deals with compensating the emissivity of the body under study and the reflected temperature (which is associated with the reflected radiation). Real temperature cannot be read on those elements whose reflectivity is high or whose reflection is diffuse. In construction, most of the materials have a high emissivity (approx. 0.9), thus the apparent temperature provided by compensating for a high emissivity of 0.9 would be very close to the real superficial temperature of an element. This is the case of concrete as material of interest.

The thermographic camera allows:

- to control a large surface. A temperature map of the element under study can be obtained by means of thermographic imaging processing software (Figure 13)
- to continuously monitor the temperature of the concrete surface

Furthermore, by knowing the thermal properties of the element (thermal conductivity, thermal inertia, etc.) models can be developed, which from the measured temperatures of the concrete surface by infrared thermography will allow determining the temperature at a given distance of the element.

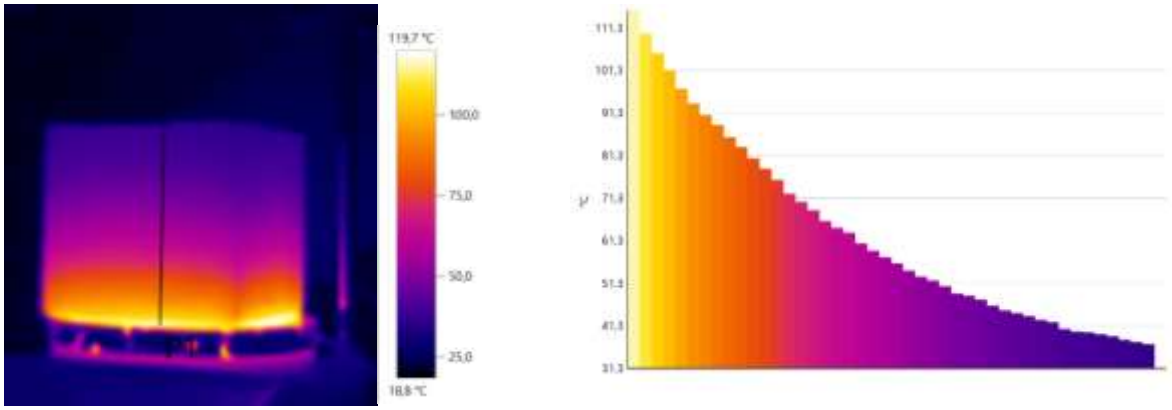

Figure 13. Thermographic image of a concrete specimen that was subjected to a temperature gradient.

The surface temperature can also be obtained with an infrared thermometer, which is based on the same principle as thermographic camera. However it does not convert the signal into an image but provides a single temperature data. This would then be an apparent temperature, as the emissivity value of the body has not been compensated. In this case the measurements are made discontinuously.

2.3. NDT methods and sensors to measure chemical parameters of concrete

2.3.1. Chlorides

Potentiometric sensors have been used for the detection of chlorides in reinforced concrete structures. These sensors, usually made with Ag/AgCl electrodes, are based on the measurement of the sensor potential versus a reference electrode. The changes in these values are related to the chloride content in the concrete matrix. The response of these sensors is affected by parameters such as presence of water and other ions, temperature or pH. The long-term stability of this type of sensors is the main weakness of in-situ application.

Another technique to detect the presence of chlorides on-site in reinforced concrete structures is the use of voltammetric sensor systems (Figure 14). In these sensors, a non-steady voltage signal is applied, achieving a current response associated with electrochemical phenomena in which, for example, chlorides, oxygen and humidity are involved. In addition, the electric current response depends on the type of sensor used. Thus, with a different type of sensors and by means of statistical multivariate analysis of the signal, is possible to isolate the different processes and identify some ions. Practical experience in long-term is still needed.

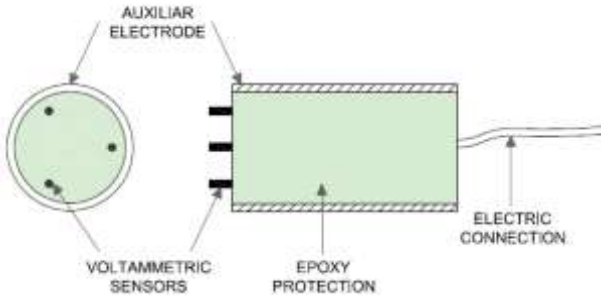

Figure 14. Voltammetric sensor system.

Therefore, through the voltammetric sensors embedded in reinforced concrete structures, it is possible to detect:

- the presence of chlorides.
- the changes in the activity of free chlorides into the concrete matrix.

2.3.2. pH

Various types of sensors can be used to estimate the pH of the concrete, such as sensors based on fluorescence fibre optic or potentiometric sensor based on the metal-metal oxide.

pH sensor based on fluorescence fibre optic

This type of sensor is suitable for the high alkaline pH region of 10 to 13. The fluorescence intensity of a dye (e.g. based on coumarin imidazole) that is chemically fixed to a carrier substance changes with the pH value. The polymeric compound is attached to an optical fibre which introduces the irradiations and leads the fluorescence intensity to an electronic spectrometer for evaluation. The sensoring part, i.e. the polymer compound positioned at the rear end of the wire, can easily be embedded in any concrete structure at any position intended. Long-term stability and low cross-sensitivities (i.e. to other ions except for hydroxide) make such type of sensor applicable for real-scale durability monitoring as well.

Potentiometric pH sensor based on metal-metal oxide

This sensor has been used in several laboratory experiences but there are not examples of long-term continuous monitoring. The electrical response of theses sensor is affected by temperature, water presence or other ions.

2.3.3. Aggressive ion detection through embedded probe sensors

By means of indirect measurements, such as with amperometric or potentiometric sensors placed at different depths, information about the changes in the cover of the rebar related to the chemical environment due to aggressive ion penetration, such as chlorides, pH changes or sulphates, can be detected. These sensors are usually of galvanic type with a pair of electrodes of varying degrees of nobility (different half-cell potential for the specific local environment). The aggressive agents as chlorides or carbon dioxide diffuse through the concrete and reach the sensor, forming a macrocell between the less noble metal (anode) and the more noble metal (cathode) and an increase in the electrical current occurs. The measured current intensity between the electrodes of each pair with an ammeter can be

associated with the presence of aggressive ions that trigger the aggressive ion penetration. However, the device does not identify the type of aggressive.

The sensor consists of several pieces of steel (anodes) located at different depths together with a stainless steel cathode (Figure 15). These systems can be useful to monitor chloride ingress or pH changes in the concrete cover, anticipating its arrival at the rebar. When sensor corrosion starts, the corrosion potential or the current between anodes and cathode will increase significantly. The rebar corrosion risk could be also identified if an embedded reference electrode for corrosion potential is placed near the sensors. These sensors can be used in the laboratory and real structures.

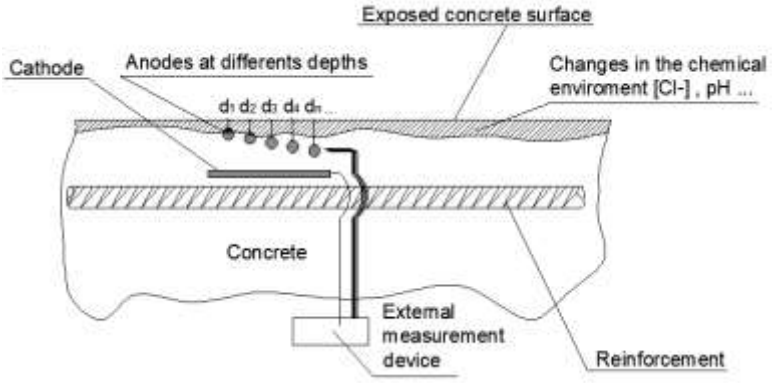

Figure 15. Amperometric sensor system.

2.4. NDT methods to assess reinforcement corrosion risk

2.4.1. Corrosion potential

The E_{CORR} measurement is the most used electrochemical method to evaluate the corrosion of reinforcement. This is due to its simplicity and short execution time and type of devices used to implement the measurements. With this method, the potential difference or voltage (half-cell potential) between the reinforcing bar and a reference electrode (in contact with the concrete) is obtained, which is related to the mixed or equilibrium potential between the oxidation and reduction reactions. This measurement is particularly suitable for an initial definition of corrosion processes in the inspected structure. This information will be the basis for further investigations and it is very useful to correctly plan them.

The E_{CORR} does not quantify the mass loss of the reinforcing bar but provides qualitative information about the onset of the corrosion process, that is, the corrosion risk. Standards usually provide potential ranges representative of different corrosion activity states (Figure 16). However, the corrosion rate and E_{CORR} depend on the oxygen and water availability at the surface of the steel and, therefore, these limits can vary greatly depending on whether the concrete is dry or completely saturated. Standards as ASTM C876 and UNE 112083:2010 states that the threshold values proposed in the standard only serve as a reference in certain conditions, such as carbonated concrete or indoor concrete that has not been subjected to frequent wetting.

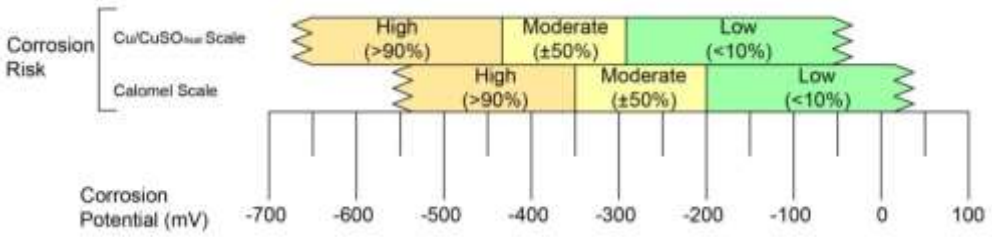

Figure 16. Relationship between the values of E_{CORR} and the probability of corrosion [UNE 112083, 2010].

The devices used for measuring the E_{CORR} are relatively easy to handle, since only one high impedance voltmeter is needed to measure the potential difference between the reinforcing bar (acting as a working electrode) and a reference electrode. The reference electrode must keep constant and reproducible potential. To carry out the test, the reinforcing bar must be connected to the positive terminal of the voltmeter. For in situ measurements on existing structures it is necessary to remove the concrete coating in a small area to make the connection or leave a permanent connection with the bar before casting. On the other hand, the reference electrode is connected to the negative terminal and in practice, frequently a wet sponge is placed between the reference electrode and the concrete surface (Figure 17, left). For measurements in the laboratory or in situ, Calomel (SCE), Ag/AgCl and $Cu/CuSO_4$ electrodes are used as reference electrodes since they are the most reliable, although they require periodic maintenance.

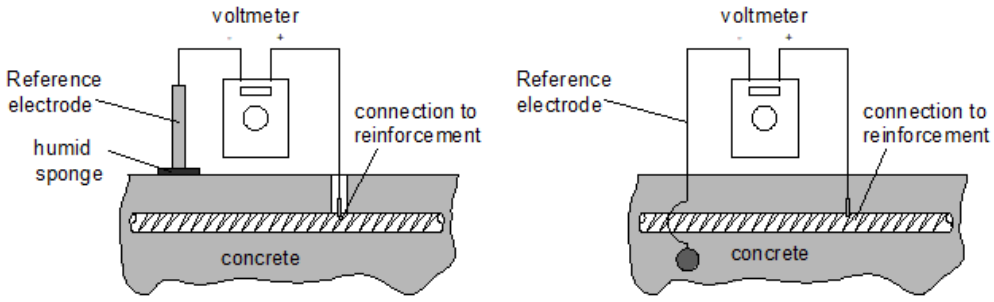

Figure 17. Scheme for corrosion potential measurements. Left, measured in situ with an external reference electrode and right, with the embedded one.

It is also possible to perform this type of measurement using embedded electrodes and permanent connection with reinforcing bars (Figure 17, right). If the reference electrode is embedded, since it is not possible to perform maintenance, specific reference electrodes must be used, the most common one being Mn/MnO_2 or Ag/AgCl.

Finally, it is necessary to take into account that changes in the concrete moisture content can significantly influence the results. It is highly recommended to complement this test with resistivity tests on the concrete cover. There are other factors that can introduce significant variations in the measurements such as carbonation processes, the presence of chlorides or the reduction of oxygen content (potentials change towards more negative values). The continuous monitoring system can be applied when using embedded reference electrodes.

2.4.2. Corrosion rate

This parameter provides quantitative information about the reinforcement corrosion kinetics. The corrosion rate measurements allow the calculation of the bar section loss per time unit, expressed in µm/year assuming that homogeneous corrosion occurs. The most common techniques to monitor the corrosion rate are electrochemical

techniques, which consist of the polarization of the reinforcing bars by forcing a small electrical current. This signal is analyzed and the Polarization Resistance (Rp, Ω) or the Current Intensity (Icorr, A) is obtained.

The methods usually employed are based on voltammetric (sweep or pulse voltammetry) or galvanometric (galvanostatic pulses). In the first case, a voltage is applied and the response current is measured; in the second case, a constant current is forced and the voltage is measured as a response. Both of them are measured versus time.

The application of all these techniques actually provides the density of corrosion current, which is the electrical current per unit surface area of the rebar onto which the corrosion processes are taking place. This parameter is directly related to the corrosion rate by the ASTM G102 or UNE 112072 standards through the following equation:

$$V_{CORR} = 11{,}6\, i_{CORR} \qquad \text{eq. (2)}$$

where i_{CORR} is the corrosion current density (µA/cm^2) and V_{CORR} is the corrosion rate (µm/year), which represents the rebar diameter loss per time unit, and is proportional to the loss of metal per unit surface area per unit time.

One of the reference methods for laboratory measurements is based on the Tafel equation. In this method, a broad potential sweep is applied around the corrosion potential (up to ± 150 mV). Then, from the obtained polarization curves (ΔV- ΔI) the corrosion current density is determined. To obtain correctly the Tafel slopes, the potential sweep must be carried out in two stages, one for the anodic branch and another one for the cathodic branch in order to recover the kinetics equilibrium after the polarization. The large polarizations of the rebar made this method not suitable as NDT, limiting its use almost exclusively to laboratory works.

An alternative to the Tafel method is the Linear Polarization Resistance (LPR) method. This method applies a voltage sweep of a smaller range (± 10 mV or ± 30 mV). In this way, the measuring time is reduced considerably and the rebar surface is almost not altered that allow the NDT use. This is the most common technique, both in laboratory and for in-situ applications, and most commercial devices exist based on this method. The procedure considers the polarization curves ΔV-ΔI as linear in the proximity of the corrosion potential and its slope (ΔV/ΔI), usually known as polarization resistance (R_p), is related to the corrosion rate with the following equation:

$$i_{CORR} = \frac{B}{R_p} \qquad \text{eq. (3)}$$

where *B* is a constant which may vary from 12 to 52 mV, however for rebars embedded in concrete value of 26 mV is the common criteria used. To determine R_p, some commercial devices apply short galvanostatic pulses instead of the voltage sweep.

In both methods, the surface of the reinforcing bar that is being polarized should be known in order to calculate the corrosion current density. To address this issue in real structures, some commercial devices include a system to confine the electric field in a specific area of the rebar (guard ring) (Figure 18).

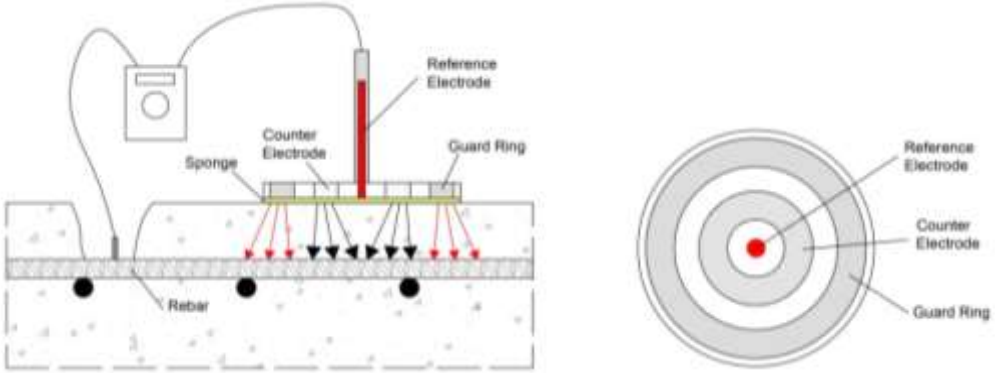

Figure 18. Standard configuration of guard ring based commercial devices for corrosion rate measurements.

Another alternative is the use of corrosion sensors, small probes with a known surface, embedded in the concrete matrix close to the reinforcement bar level (the measurement is made on the sensor). On the other hand, if the sensors are connected to an automatized measuring system, which can transmit the data remotely, a continuous monitoring can be carried out even in the non-accessible parts of the structure.

Table 2. includes the reference values of V_{CORR} and i_{CORR} which are used to state the rebar corrosion risk.

Table 2. Limit values for i_{CORR} and V_{CORR} to identify corrosion levels.

Corrosion level	i_{CORR} ($\mu A/cm^2$)	V_{CORR} (μm/year)
High	≥ 1.0	≥ 11.6
Moderate	0.5 – 1.0	5.80 – 11.60
Low	0.1 – 0.5	1.16 – 5.80
Negligible	≤ 0.1	≤ 1.16

2.5. NDT to measure mechanical parameters of reinforcement

2.5.1. Reinforcing bar deformation

The reinforcement deformation can be obtained by analyzing the deformation in the concrete or directly implementing strain measuring devices onto the reinforcing bars themselves, such as linear variable differential transformer (LVDT) or strain gauges (SG). Their working principle has been described previously in section 2.1.4.

The installation of strain gauges directly on the surface of the bars requires a specific procedure. This procedure consists of the previous preparation of the surface by machining the ribs, so the strain gauges can be attached on a planar and smooth surface. After that, the strain gauges are glued to the bar by using specific adhesives (cyanoacrylates). Once the adhesive has hardened, a strongly adhering kneadable putty material is used to protect both the sensing surface of the strain gauges and the electric connections (Figure 19).

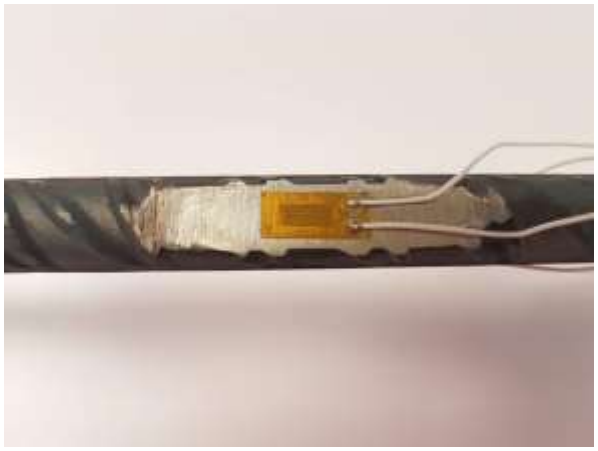

Figure 19. Strain gauge.

3. Non-Destructive techniques verification and reliability according to UHDC and XA/XS scenarios

The reliability of the non-destructive techniques described in section 2 has to be verified when Ultra-High Durability Concretes (UHDC) are employed. Their higher compactness, higher content of anhydrous cement particles or the high content of steel fibres, very often added, could affect the measurement or even the applicability of some NDT. Therefore, it is important to ensure that these techniques on whose measurements the durability design models are based on CC constructions are also valid for UHDC constructions.

Considering the damage that might occur in the XA and XS scenarios considered in this project, validation tests have been carried out to verify the sensitivity and reliability of some NDTs for its use in UHDC. The tests performed are listed in Table 3.

Table 3. NDT for UHDCs test in the laboratory and partner involved.

Durability parameter	Concrete							Reinforcement	
	Mechanical			Physical		Chemical		Corrosion risk	
	Ultrasonic pulse velocity	Acoustic emission	Deformation	Gas permeability	Electrical resistivity	Chlorides penetration	pH	E_{CORR}	i_{CORR}
Technique application	external	external	external-embedded	external	external	embedded	embedded	external	external-embedded
UHDC	XA, XS-offsh	XSma	XS-offsh	XS-offsh	XA, XS-offsh	XS-offsh	XS-offsh	XS-offsh	XS-offsh
Partner concrete production	POLIMI, UPV	BGU	UPV	UPV	POLIMI, UPV	UPV	UPV	UPV	UPV
Partner involved	CSIC-UPV	BGU	UPV	UPV	CSIC-UPV	UPV	UPV	CSIC-UPV	CSIC-UPV

XA: XA chemical attack, XS-offsh: XS-Mediterranean offshore, XSatl: XS-Atlantic, XSma: XS-Mediterranean aerial scenarios

The different concretes used in the characterisations are those designed and selected in D4.2 and D5.1. The dosage of these concretes are included in sections 2.1.1 and 3.1.1 of Deliverable 5.1, and the nomenclature used is as follows: CA: crystalline additive, ANF: Alumina nanofibres, CNF: cellulose nanofibrils, CNC: cellulose nanocrystals, CN: cellulose nanofibrils and nanocrystals (equally shared).

- UHDCs for XA chemical attack:
  - XA-CA: reference mix (with CEM I), 4.8kg/m^3 CA
  - XA2-CA: reference mix (with CEM III), 4.8 kg/m^3 CA
  - XA-CA+ANF: 4.8 kg/m^3 CA, 0.25% ANF
  - XA-CA+CNF: 4.8 kg/m^3 CA, 0.15% CNF
  - XA-CA+CNC: 4.8 kg/m^3 CA, 0.15% CNC

- Concretes for XS Mediterranean offshore:
    - CC: conventional concrete (f_{ck} ≈ 25 MPa)
    - HPC: high strength concrete (fck ≈ 90 MPa)
    - XS1: UHDC reference mix (offshore)
    - XS2: UHDC reference mix (mussel farm)
    - XS1-CA+ANF: same dosage as XS1 and 0.8% CA, 0.25% ANF
    - XS2-CA+CN: same dosage as XS2 and 0.8% CA, 0.15% CN
- Textile reinforced UHDC (TR-UHDC) for XS Mediterranean aerial:
    - REF: reference mix
    - CA: reference mix and 0.8% CA
    - CA+ANF: reference mix and 0.8% CA, 0.75% ANF

3.1. NDT for mechanical evaluation of UHDC

3.1.1. Ultrasonic pulse velocity

To study the sensitivity of this technique with UHDCs, the following concrete conditions have been analyzed:

- effect of type of concrete
- effect of ageing
- effect of cracks

Testing method

Direct and indirect ultrasonic pulse methods were employed following the standard procedure described in EN 12504-4 “Testing concrete. Part 4: Determination of ultrasonic pulse velocity”, applying a gel to the transducers to ensure good acoustic contact because of non-smoothness of the concrete specimen surface. The measurements were carried out at 2 and 6 months by CSIC on cylindrical uncracked specimens with a diameter of 100 mm and a height of 50 mm obtained from UHDCs designed for XA chemical attack and XS-Mediterranean offshore scenarios, and from CC and HPC. The samples were pre-saturated under vacuum with deionized water. On the other hand, UPV and CSIC determined the ultrasonic pulse velocity on 100x150x50mm prismatic specimens with three levels of cracking in XS Mediterranean offshore scenario. The testing arrangements used, are shown in Figure 20 for direct measurement and that shown in Figure 1 for indirect.

Figure 20. Ultrasonic pulse velocity set up.

Sensitivity of the technique

a) Effect of type of concrete and ageing

Figure 21 shows that with the ultrasonic pulse velocity is possible to determine differences in UHDCs. Results show small differences with UHDCs qualities, from XA chemical attack and XS-Mediterranean offshore scenarios, regardless of types of cement and nanoadditions introduced. These values are in the order of $5x10^3$m/s for the two studied ages, 2 and 6 months. However, some differences are observed between UHDCs without additions and HPC and CC, the measured ultrasonic pulse velocity values being slightly higher for HPC and lower for CC as expected, demonstrating the sensitivity of the technique. The influence of nanoaddition incorporation into the UHDC has been also appreciated in some cases, where a slight decrease in the ultrasonic pulse velocity is observed. In the same way, changes in strength and porosity of the concretes were also observed.

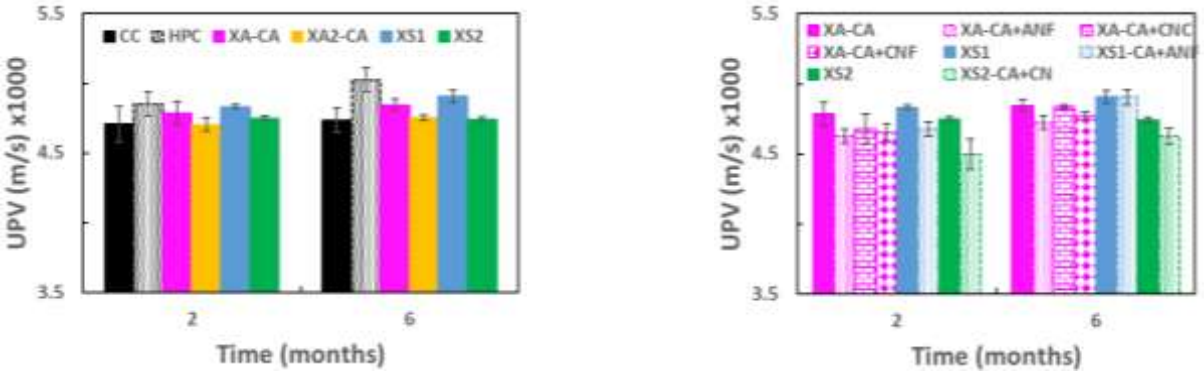

Figure 21. Effect of concrete type and ageing.

b) Effect of the cracks

The presence of cracks was also appreciated by the ultrasonic pulse velocity with both direct and indirect methods (Figure 22). Crack damage and the size of the cracks have a significant influence on the transport of the wave for XS specimens, the rates being lower in cracked concretes. The detection of the presence of cracks is demonstrated with indirect UPV (figure 22 right), where lower rates are measured in crack concretes, being lower with UHDC wth respect to HPC.

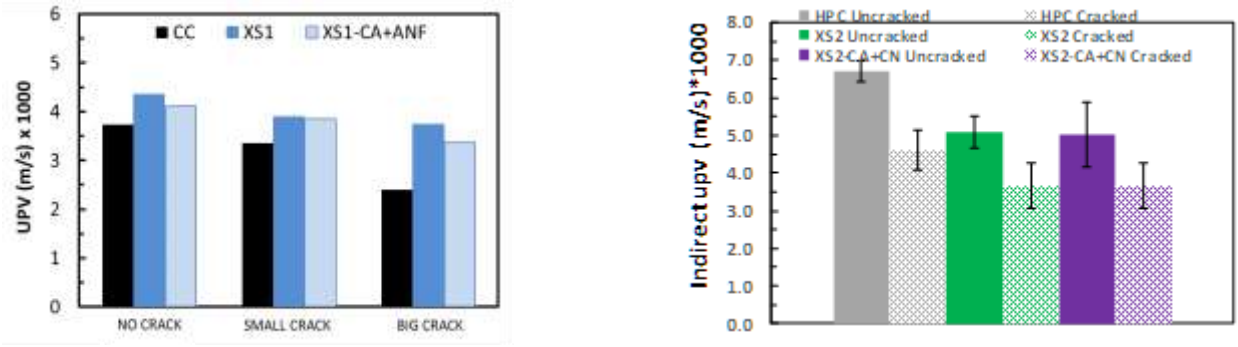

Figure 22. Effect of cracks. Left) direct method. Right) indirect method.

A study of the evolution of the cracks through the concrete was also carried out (Figure 23). In general, the ultrasonic pulse velocity decreases with the crack, being lower for larger than for smaller cracks; but also, as can be seen in Figure

23, it is higher in the inner zone (center) due to the variation of the crack widths along its development length, being narrower close to the tip and close to the reinforcement.

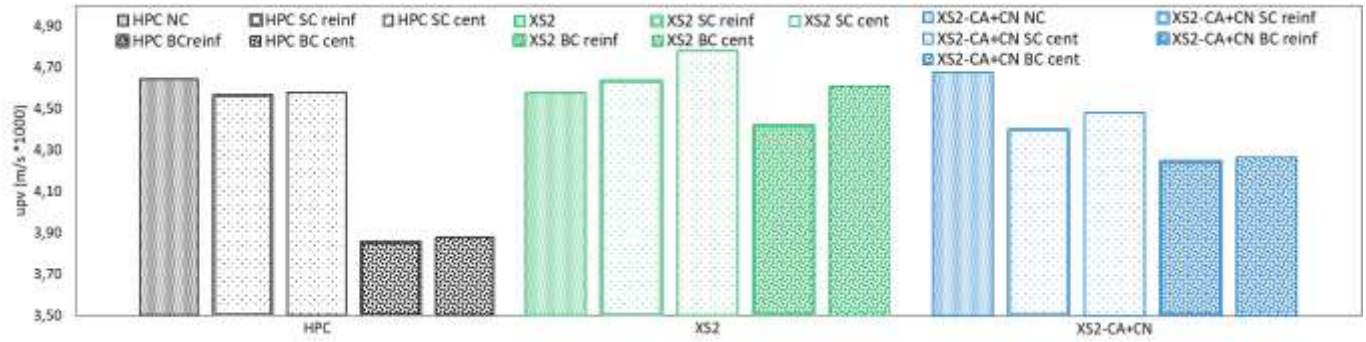

Figure 23. Effect of the evolution of cracks in HPC, XS2, and XS2-CA+CN concretes. NC: No cracks, SC: small cracks, BC: big cracks, cent: center, and reinf: reinforcement.

The main conclusions drawn from experiences on the ultrasonic pulse velocity technique are the limited sensitivity to Ultra-High Durability Concrete differences and its significant sensitivity to damage state with crack. Both methods, direct and indirect have demonstrated good sensitivity and applicability.

3.1.2. Acoustic emission

Acoustic emission measurements were performed on three types of textile reinforced concrete elements (TR-UHDC), as discussed in WP4. The samples were prepared from each mixture type; each sample contains one layer of epoxy impregnated carbon fabric located in the center while each fabric layer contains three reinforcing yarns along the loading direction. The dimensions of each TR-UHDC specimen are: length 300 mm, width 25 to 30 mm and thickness 9.5 to 11 mm. The TR-UHDC specimens were subjected to saturated sodium chloride solution: continuously immersed (Cl) or subjected to 24h wet/dry cycles (WD) and compared to conventional curing in tap water (TW). Such aggressive XS condition and cycles of hot and dry climate are meant to simulate the environmental conditions experienced by the water reservoir tower in Malta.

The specimens were tested under tensile loading. Four acoustic emission sensors were located along the specimen length during the tensile tests as shown in Figure 24. Deformation or a crack produced in the specimen under tensile loading becomes a source of a mechanical wave, this is termed as an *event* and was recorded by the Acoustic emission (AE) sensors.

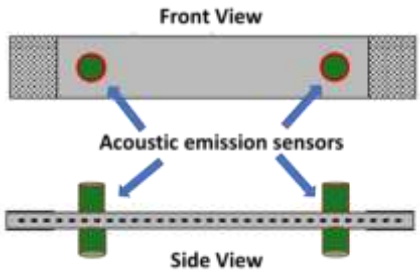

Figure 24. Schematic of acoustic emission system sensors placement on the specimens.

Absolute energy (abs energy) of such waves detected by AE sensors gives a measure of how intense the crack is. Cumulative abs energy provides a measure of the extent of defects. Cumulative abs energy with Load history for typical specimens from REF, CA, and CA+ANF exposed to tap water is presented in Figure 25. Within the Multiple cracking load range of the matrix 500 to 2500 N, the REF system released highest energy followed by CA+ANF. CA system showed minimal deformation in this load range. This illustrates that there are fewer deformations or defects in CA system, followed by CA + ANF and REF. The addition of CA to the matrix could have enhanced the strength by minimizing the deformations and number of cracks in the specimen.

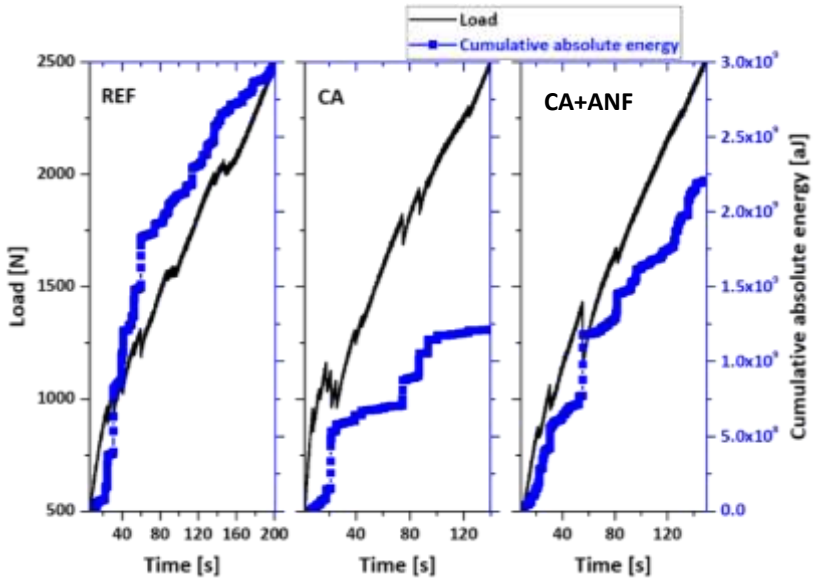

Figure 25. AE results of cumulative absolute energy of REF, CA and CA + ANF TR-UHDC systems immersed in tap water.

REF, CA and CA+ANF TR-UHDC samples followed the same AE trend after continuous exposure to NaCl saturated water (Figure 26). However, in all the three systems subjected to NaCl saturated water, the cumulative abs energy is nearly doubled as compared to those cured in tap water. The trend is quite different when these specimens were exposed to dry and wet cycles in NaCl saturated water, CA system showed the highest cumulative energy followed by REF while CA+ANF system was the least (Figure 27). A comparison of the average cumulative absolute energy results of all the three TR-UHDC specimens exposed to the three curing procedures are presented in Figure 28. Under dry/wet conditions, the CA+ANF system is least affected.

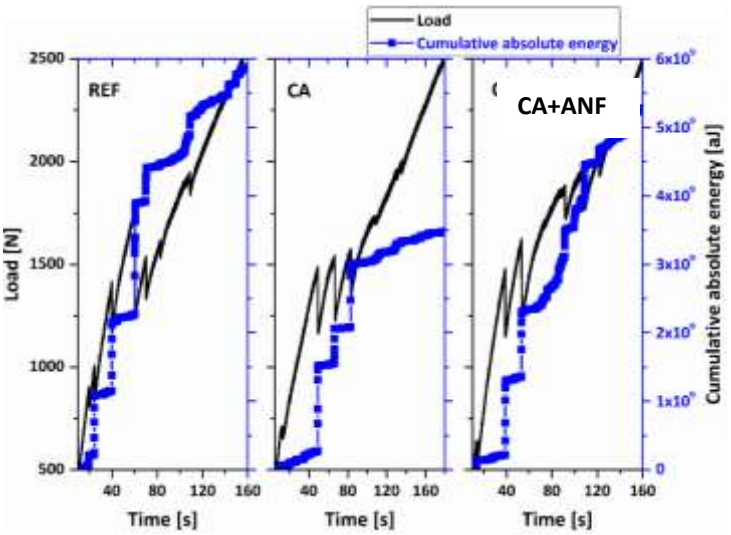

Figure 26. AE results of cumulative absolute energy of REF, CA and CA + ANF TR-UHDC systems continuously exposed to NaCl saturated water.

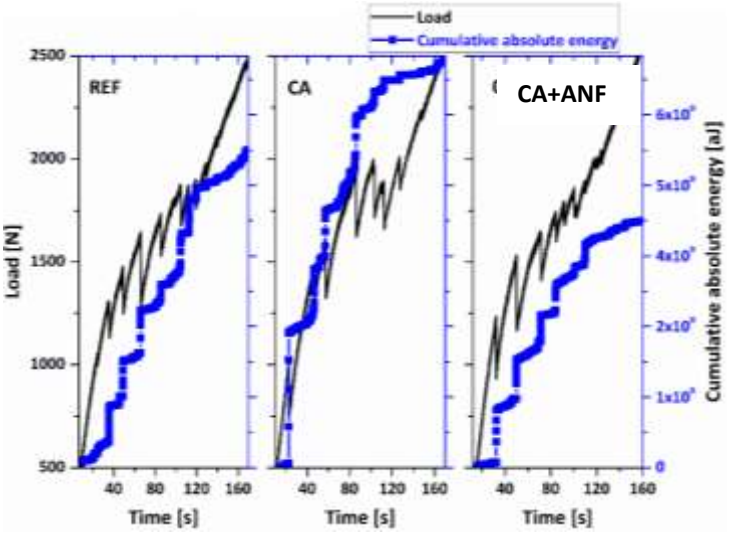

Figure 27. AE results of cumulative absolute energy of REF, CA and CA + ANF TR-UHDC systems exposed to dry and wet cycles in NaCl saturated water.

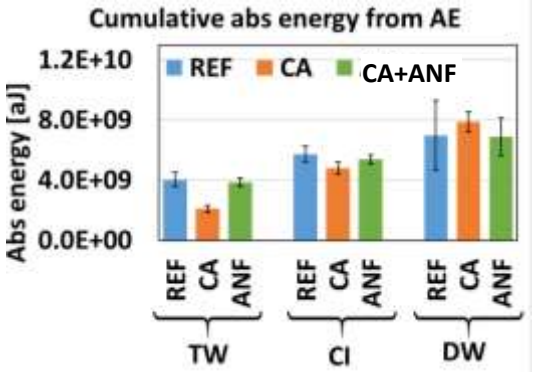

Figure 28. Average AE results showing cumulative absolute energy of of REF, CA and CA + ANF of TR-UHDC systems exposed to all three curing procedures (continuously exposed to saturated NaCl solution (Cl), subjected to 24h wet/dry cycles (WD) in NaCl solution and in tap water (TW)).

Amplitude is one of the important parameters obtained from the AE measurement. Moving average of Amplitude of 400 points against time with load history is presented in Figure 29 for typical specimen of REF, CA and CA+ANF systems exposed to the three different investigated curing conditions (TW, Cl, DW). In all cases, it is observed that during the multiple cracking of the matrix higher amplitude values are registered and in the later loading stage intensity of the moving average of amplitude decreases. This parameter can be used for identifying the damage in the specimen.

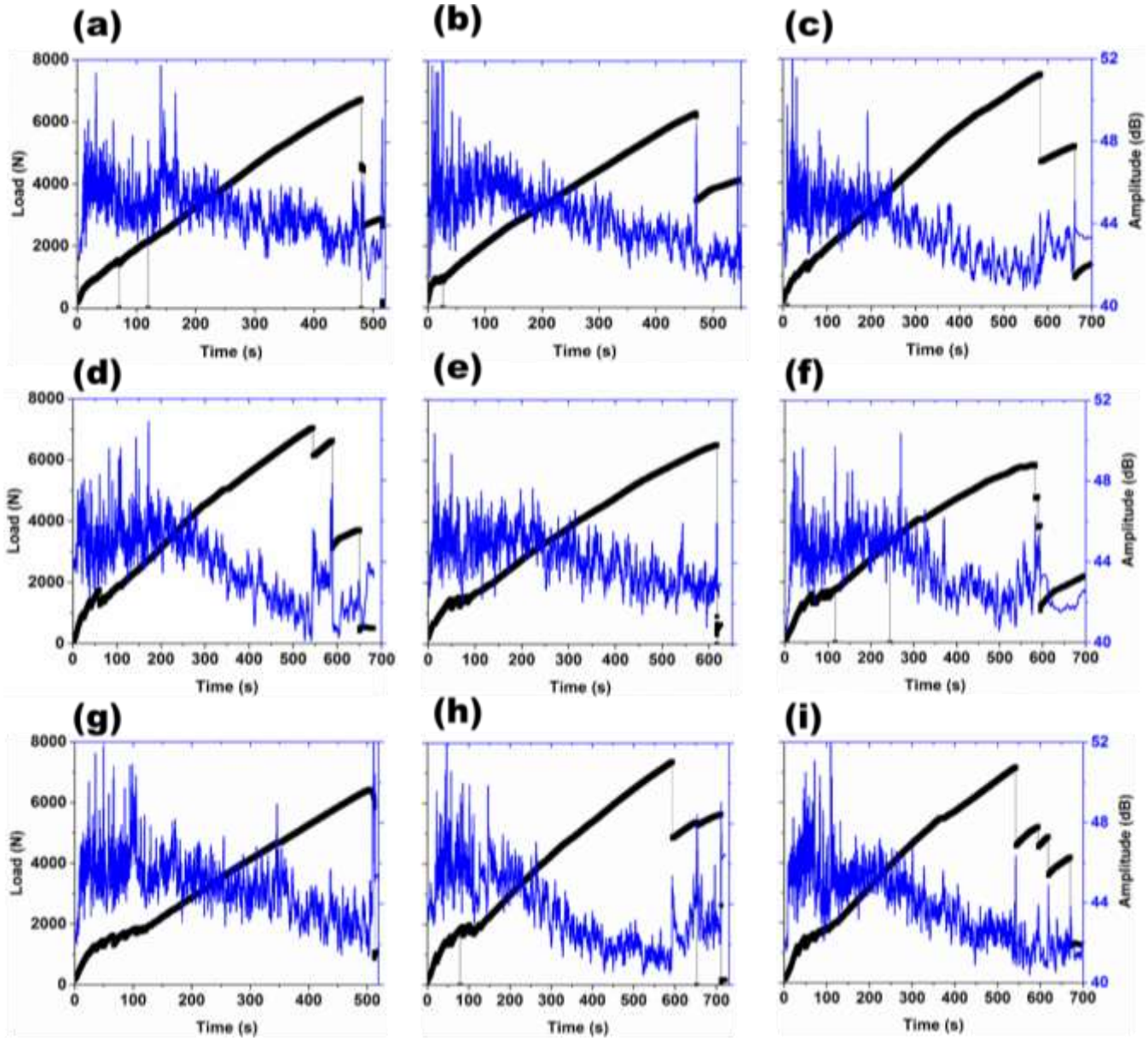

Figure 29. The moving average of AE amplitude of 400 points vs along with the load history of specimens exposed to tap water (a) REF, (b) CA, and (c) CA+ANF; specimens exposed to NaCl saturated water (d) REF, (e) CA, and (f) CA+ANF; specimens exposed to dry/wet cycles (g) REF, (h) CA, and (i) CA+ANF.

Further, Figure 30, 31 and 32 show the absolute energy with the load history. It can be clearly observed that the first load drop, which is the first macro crack in the matrix, is accompanied by high value of abs energy as indicated by orange rectangle. This shows that irrespective of the mix design and exposure conditions, AE system can be used to

detect the cracks and monitor the health of concrete structures, including the UHDC ones investigated in the project ReSHEALience.

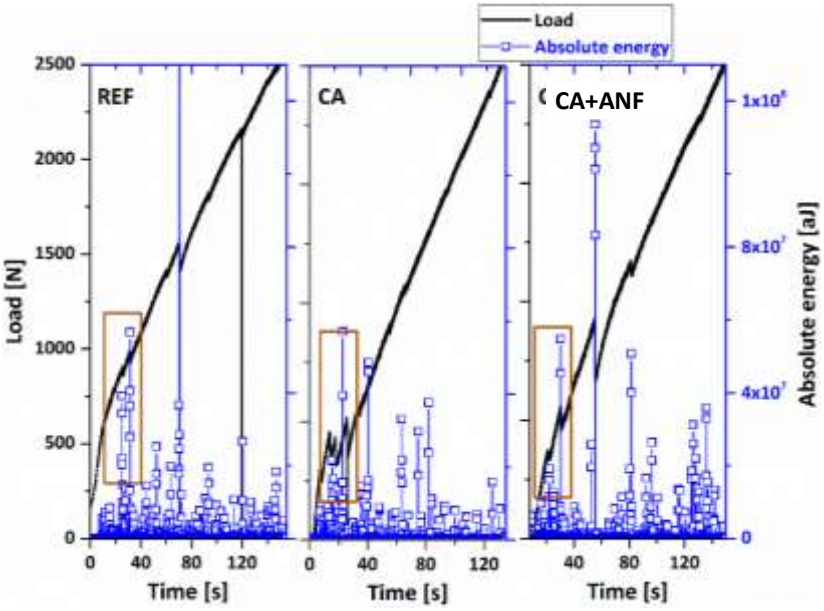

Figure 30. Abs energy vs time along with the tensile load history of specimens exposed to tap water. First crack can be detected by abs energy value indicated in the orange rectangle.

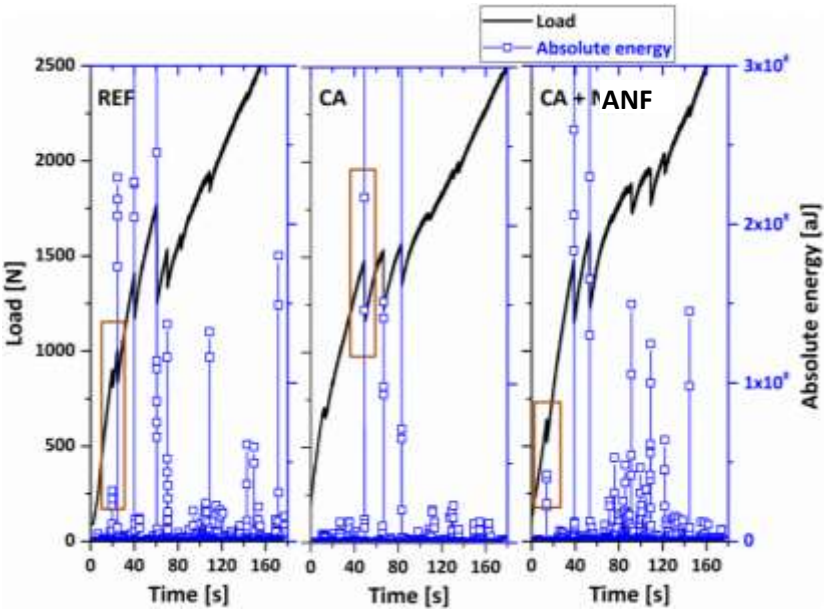

Figure 31. Abs energy vs time along with the tensile load history of specimens exposed to NaCl saturated water. First crack can be detected by abs energy value indicated in the orange rectangle.

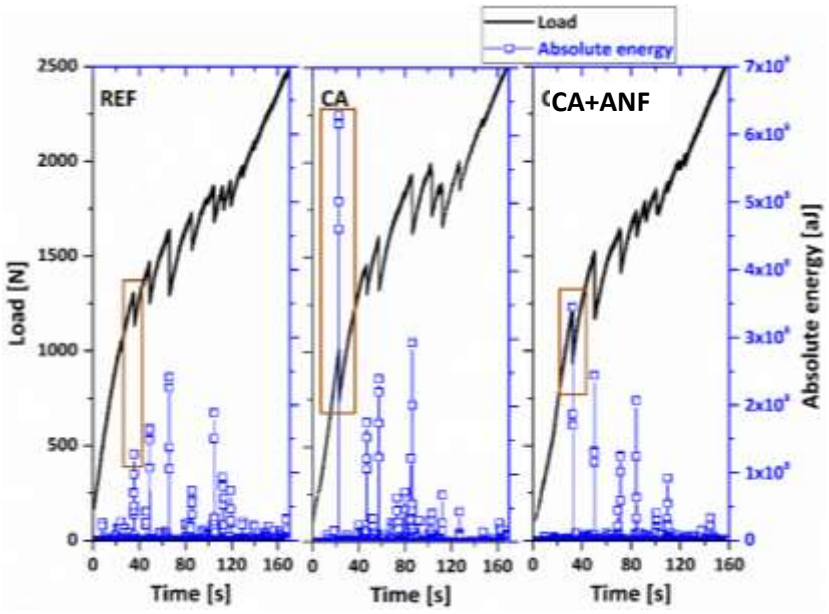

Figure 32. Abs energy vs time along with the tensile load history of specimens exposed to dry/wet cycles. First crack can be detected by abs energy value indicated in the orange rectangle.

Plot of the average frequency vs. the rise angle can reveal the nature of crack occurring in the matrix, including cracking [Ohno and Ohtsu, 2010] as indicated in the schematic presentation in Figure 33a**.** In the initial loading period the deformations in the specimens are predominantly tensile in nature rather than shear. In other words, tensile stresses are dominant at the beginning of loading before the occurrence of macro cracks in the specimen. From this point and further a multiple cracking behaviour is the dominant mechanism; thus shear stresses are developed at the interface between matrix and textile. Thus, when the specimens are under tensile loading, at the initial loading the AE signals are corresponding to tensile stresses, once the multiple cracking occurred in the specimen, the AE signals are mostly corresponding to shear stresses. This behavior can clearly be seen for the TR-UHDC specimens presented in Figure 33b,c for CA+ANF sample exposed to dry/wet cycles, showing the average frequency vs. the rise angle. Two different ranges of frequency are observed which corresponded to 0 - 800 N loads and 0- 2500 N loads. In the initial loading phase (up to 800 N) the stesses in the specimen are mostly tensile (Figure 33b); from this point i.e., after the occurrence of the first crack (above ≈ 800 N) AE signals corresponding to shear stresses are dominant (Figure 33c). Similar behavior was obtained in all tested TR-UHDC series, showing the ability to discriminate the nature of cracking by the AE measurements.

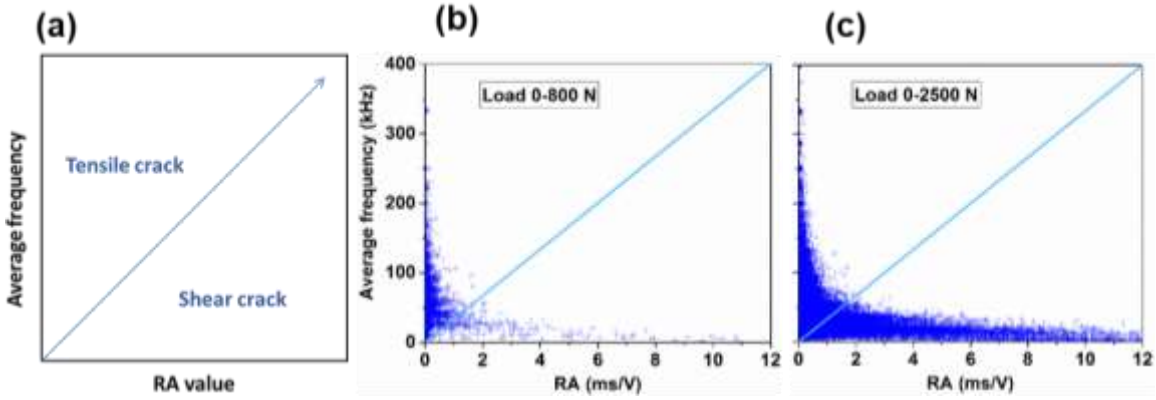

Figure 33. (a) Schematic illustration indicating the tensile and shear cracks, (b and c) CA+ANF specimens exposed to dry/wet conditions in the load range of 0-800 N and 0-2500 N respectively.

AE analysis shows that when REF, CA and CA+ANF systems are exposed to tap water or continuously exposed to NaCl saturated water, the CA system was least affected. Therefore, in those curing conditions CA-based UHDC is preferred. When the same specimens were exposed to NaCl saturated water under dry/wet cycles (in/out of NaCl saturated water), CA+ANF is least affected, thus for these type of environmental condition CA+ANF system is preferred.

The main conclusion with respect to the AE NDT method is that it can be used to detect the crack damages of structural elements made with UHDC and monitoring their health.

3.1.3. Surface concrete deformation

The viability of using strain gauges to measure deformation was verified by UPV with UHDC. Conventional strain gauges were used and glued to the surface of the concretes. The selection of strain gauges was made according to the particle size of the aggregate. Usually, the size of the grid should exceed 4 times the particle size of the aggregate of the concrete onto which the strain gauge is attached. Because in the UHDC only fine aggregates are used, also strain gauges that are not employed in conventional concretes can be reliably used.

Tests have been made on XS2 concrete specimens using strain gauges with grid both 6 and 50 mm long with equivalent results (Figure 34, left). As it is easier to work with smaller strain gauges, the ones with a grid of 6 mm have been chosen (Figure 34, right). Two different adhesives have been employed: a bicomponent cold-curing glue and a cyanoacrylate based adhesive (super-fast curing). As both exhibit optimal adhesion, the cyanoacrylate based adhesive has been selected because it features an easier application and faster curing.

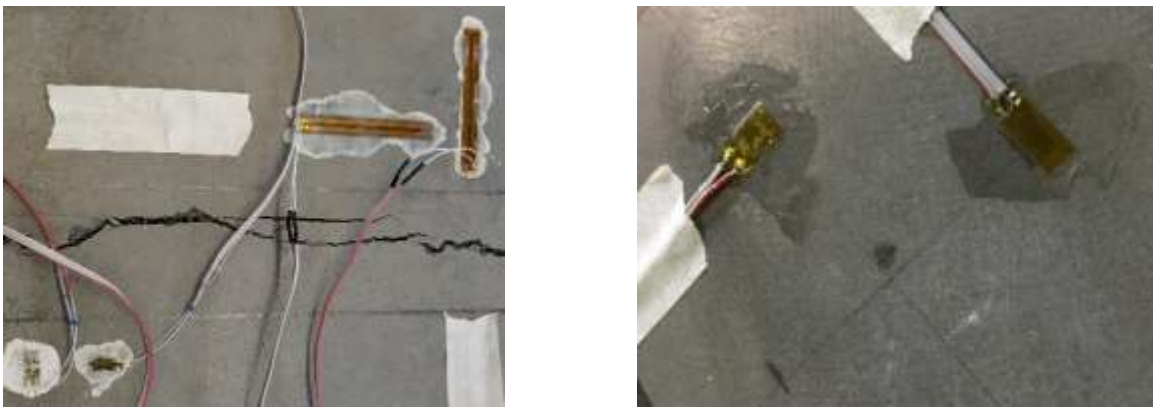

Figure 34. Strain gauges adhesives tests.

As an example of the performance of the short strain gauges (6 mm grid), Figure 35 plots the deformation under a load applied in the center of a 25x75 cm slabs at the 3 subsequent increasing levels (8.3, 8.7 and 11.1 kg). The measurement was set in a half-bridge configuration. This measurement procedure allows measuring variations in the range of µm/m. A good response to these measurements can be observed.

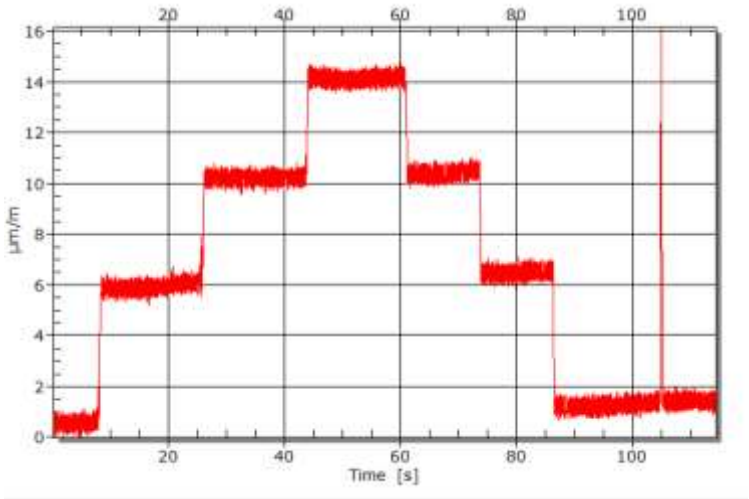

Figure 35. 6 mm grid strain gauges test in XS2 concrete.

The main conclusion derived from the use of strain gauges to detect concrete deformations is that this NDT is sensitive and valid for UHDC. The measurement can also be taken in a continuous mode and operate remotely using a wireless connection that allows the information to be transmitted to a control center. In environments, where the concrete is wet or under immersion, multi-layer protection of the strain gauge is absolutely essential.

3.2. Physical parameters of concrete

3.2.1. Gas permeability

Gas permeability (k_T) was evaluated in samples with different crack ranges using a PermeaTORR equipment. The test indicates both the air permeability and the depth of penetration of the air pressure. The results are displayed in Table 4 and show that cracked samples with distributed cracks have similar air permeability than uncracked traditional concrete or less air permeability despite the presence of cracks. These results also demonstrate the high durability performance of UHDCs compared to more traditional concrete types and that this NDT is valid to be used in UHDC.

Table 4. Gas permeability measures.

Type of sample	Level of crack	kT $\cdot 10^{-16} m^2$	Depth (mm)
CC	Uncracked	0.1295	18
XS2	Uncracked	0.0062	4
HPC	Beam – uncracked zone	0.0046	3
XS1	Beam – cracked zone	0.1377	18
XS1	Beam – uncracked zone	0.0004	1
XS1	Beam – cracked zone	0.1794	21
HPC	Beam – cracked zone	0.0036	3
HPC	Beam – uncracked zone	0.0051	4
HPC	Beam – cracked zone	96.4108	243

Figure 36 plots the gas permeability results, showing that for the uncracked state the higher the concrete quality (CC, HPC, XS1, and XS2) the lower the gas permeability is. In the cracked state, XS1 beams have comparable gas permeability to that of uncracked CC beams and only slightly higher than that of HPC uncracked beams. XS2 seems to have higher gas permeability than XS1.

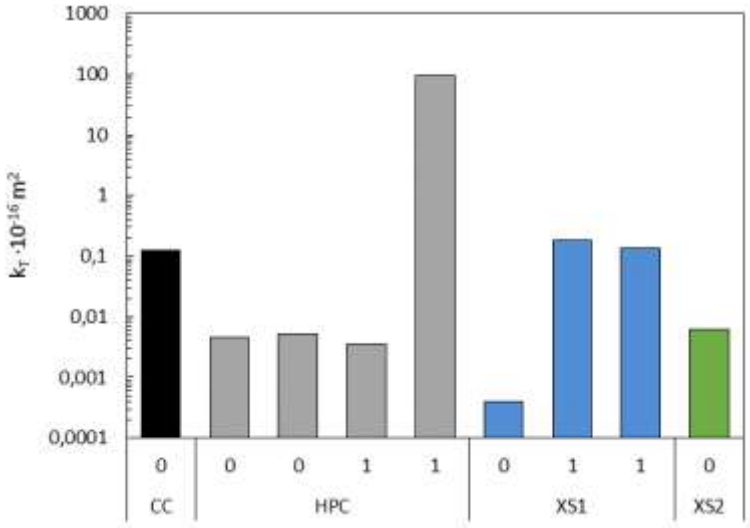

Figure 36. Gas permeability measures for each concrete type depending on the crack level (0 for uncracked, 1 for cracked samples).

The main conclusion is that the gas permeability NDT method is valid for UHDC, even in cracked state, and therefore can be used to characterize these concretes.

3.2.2. Electrical resistivity

For the study of the sensitivity of this NDT technique for its use in UHDC, the following aspects have been analyzed:
- effect of type of concrete
- effect of ageing
- effect of specimen type and size
- effect of cracks

Testing method

Resistivity was determined through two methods: 1) using the direct system (standard UNE 83988-1), by applying a uniform electric field using two stainless steel electrodes in contact with the specimen bases, and 2) indirect, using the Wenner system, as indicated in Figure 10. The tests were carried out with cylindrical specimens with 100 mm diameter and 50 mm height, from samples of 100x300 mm for concretes corresponding to XA chemical attack scenario (specimens produced by PoliMi) or 100x200 mm for concretes corresponding to XS-Mediterranean offshore scenario (specimens produced by UPV). To ensure good electrical contact between the concrete sample and the electrodes, previously moistened sponges with the same area as the electrodes were used. In order to guarantee that the applied pressure was homogeneous and repeatable, two methacrylate plates and a weight (2 kg approximately) were used (Figure 37). The samples were pre-saturated under vacuum with deionized water. Electrical resistivity was measured

at the ages of 2 and 6 months by CSIC (for XA and XS scenario specimens) and UPV (for XS Mediterranean offshore specimens). For indirect measurements, prismatic samples of 100x150x50mm with and without cracking were used.

Figure 37. Electrical resistivity set up by direct method.

To study the effect of specimen type on the measurements, the resistivity was evaluated on two types of specimens. One of them was a cylindrical specimen with a diameter of 100 mm and a height of 50 mm, and the other one was prismatic of 40x40x160 mm. In this last case, the measurement was made in two directions: a) in the longitudinal direction, using two square 40 mm side electrodes placed on the specimen heads, and b) in a cross direction, using two rectangular 40x160 mm electrodes placed on two opposite faces. These tests were performed on XS1 concrete at the age of 1 year by UPV.

The effect of the cracks was evaluated on XA UHDCs using cylinders Ø100x50 mm with 5mm deep diameter notches cut on the surface. In order to assess the cracks through the resistivity method, two measurement configurations were employed: towards the crack (direct method) and against the crack. Due to the geometry of the samples, the resistivity could not be determined; however, the resistance (R) of the concrete can be considered proportional to the resistivity as long as the contact area and the distance between meshes is maintained.

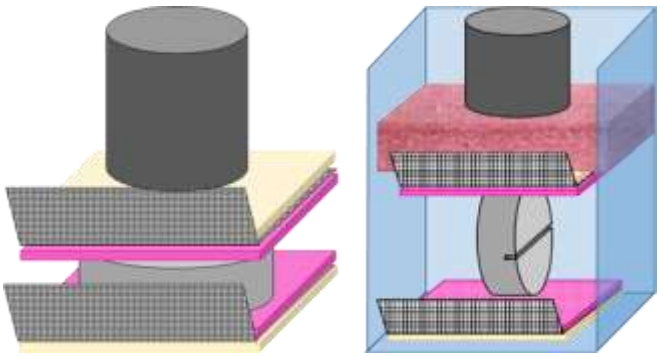

Figure 38. Resistivity/resistance measurement towards (left) and against (right) the crack.

Sensitivity of the technique

a) Effect of concrete type and ageing

In concretes designed for XA chemical attack scenario, low resistivity values (ρ_e) have been obtained for the XA-CA, XA2-CA, XA-CA+ANF, XA-CA+CNC, and XA-CA+CNF concretes, ranging from 20-30 Ωm at 60 days (Figure 39, left). After 6 months, an increase of the electrical resistivity occurs related to the progress of hydration, with values ranging

between 65 and 140 Ωm. These values remain low, most likely due to the incorporation of steel fibers into the concrete. A small difference can be observed at 6 months, where the concretes containing only the crystalline additive have slightly lower resistivity, while the combination with ANF increases this electrical resistance, indicating that the technique is able to detect differences in microstructure of the UHDCs.

In addition, ρ_e values measured at 2 months for the UHDCs designed for XS-Mediterranean offshore scenario show values between 1.4-2x10^3 Ωm, highlighting clear differences according to the concrete compositions (Figure 39, right). Changes in electrical resistivity are observed in these concretes with the incorporation of nanoadditions, with decreasing values reaching 1x10^3 Ωm. The electrical resistivity values increase with the curing time due to a decrease in the porosity as a consequence of the progress of hydration of the concrete for the XS1 and XS2 in the absence and presence of nanoadditions, reaching values around 3x10^3 Ωm. Nano-additioned mixes always providing lower values than their companion non-additioned mixes.

Electrical resistivity values are lower for HPC and CC concretes, around 650 Ωm for HPC and 60 Ωm for CC at 2 and 6 months. The electrical conductivity in the concrete is mainly due to ionic transport through the pore network and it is affected by the pore saturation (equivalent to the open porosity). CC has a more porous structure and higher permeability and therefore presents lower resistivity. The technique is sensitive to changes in the microstructure of the concretes.

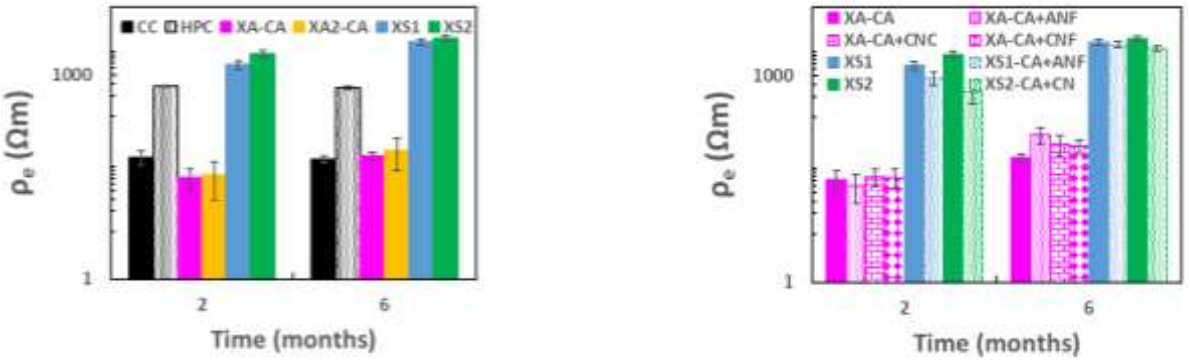

Figure 39. Electrical resistivity for the UHDCs: Left) Concretes designed for XA scenario, Right) Concretes designed for XS Mediterranean offshore scenario.

b) <u>Effect of specimen type and size</u>

As shown in Figure 40, the resistivity values are very different, even for the same concrete. The values obtained in the longitudinal direction of the 40x40x160 mm prismatic specimen are around 20% of those obtained in the 100 mm diameter cylindrical specimen. These differences can be explained as a consequence of two main reasons. On the one hand, due to the low permeability of the UHDCs, it is difficult the saturation inside of the specimen even using a vacuum system. Thus, in the larger specimens, the resistivity will tend to be greater (the saturated surface/dry surface ratio of the section is smaller). On the other hand, in small 40x40x160 mm specimens it is possible that the steel fibers are better oriented in the longitudinal direction of the specimen. This fact can favor the conductivity in that direction, obtaining resistivity values in the longitudinal direction lower than in the cross direction.

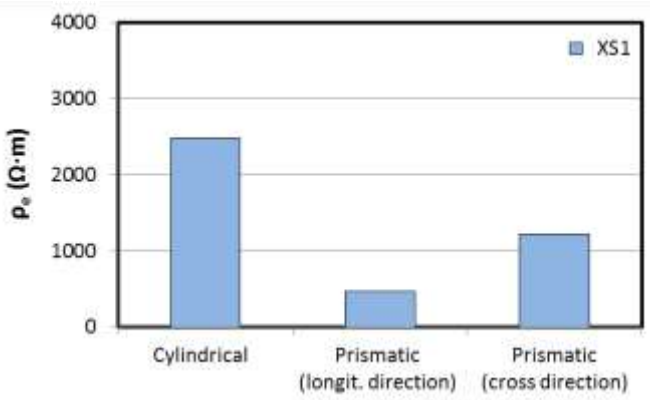

Figure 40. Effect of specimen type on electrical resistivity in UHDCs.

c) <u>Effect of cracks</u>

The resistance with direct and indirect methods was evaluated in the uncracked and cracked specimens from the concretes designed for XA scenario in permanent contact with simulated geothermal water and the proportionality between resistance and resistivity was checked. In this sense, concrete resistance values towards and against the cracks have been compared. Figure 41 shows that cracks do not affect the measurement in any configuration employed.

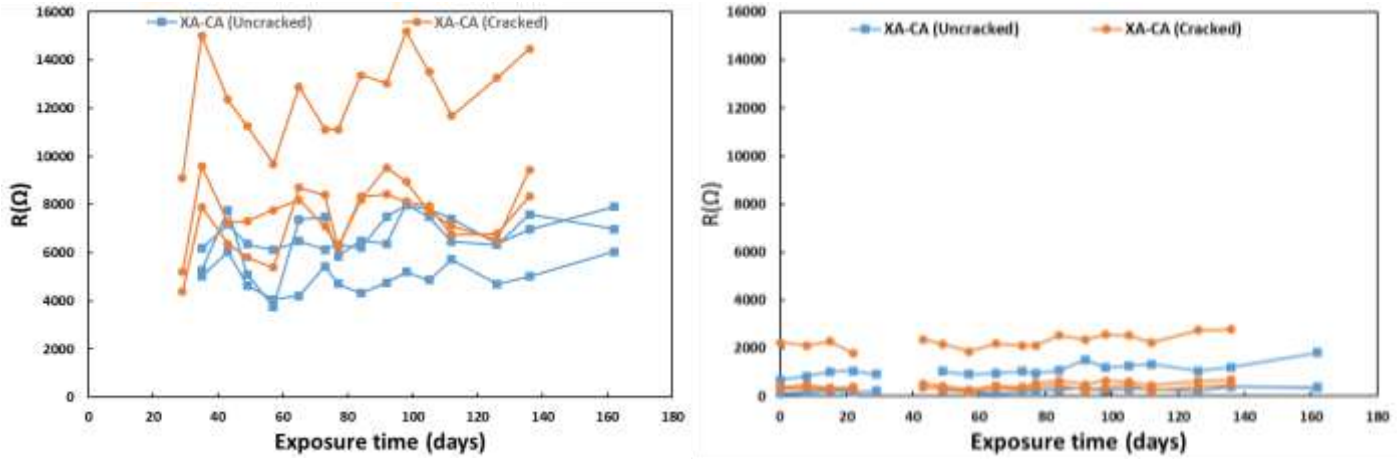

Figure 41. Evolution of electrical resistance for uncracked and cracked XA-CA specimens over time measured towards and against the crack.

In theory, the presence of cracks in a material implies a decrease in electrical resistance. However, the cracked concretes do not show the lowest R values. This behavior can be explained by wet conditions of the samples (water could conduct electricity through pores or small cracks), the limited sensitivity of the electrical resistivity test (it is not able to detect the damage in UHDC concretes) or due to the presence of fibres in these concretes, which sew the crack and therefore there are no differences in electrical resistivity measurements in both states, cracked and uncracked and in both configurations (toward and against the crack).

However, as shown in Figure 42, when the resistivity is evaluated with the indirect method (Wener method), differences are well detected between cracked and uncracked concrete and type of concrete (HPC and XS2).

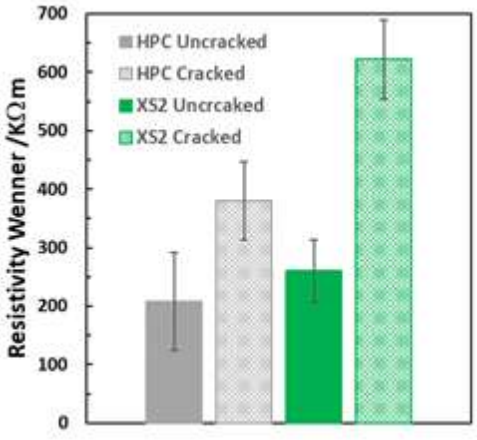

Figure 42. Wenner method resistivity for uncracked and cracked specimens.

The main conclusion for electrical resistance as non-destructive technique is that it shows a great sensitivity regarding the type of concrete and the presence of additions, and therefore can be used to characterize UHDCs. However, due to the large discrepancies observed in the results when using specimens of different shapes and sizes, it is necessary to create a specific test protocol for this type of concretes. The results have not been able to clarify the suitability of the direct method to detect cracks in UHDC concretes with high steel fibre content while using the indirect method (Wenner method) differences are well detected between cracked and uncracked concrete, being higher resistivity in cracked respect to uncracked conditions.

3.3. Chemical parameters of concrete

3.3.1. Chlorides detection

The use of silver voltammetric sensors to detect the presence of chlorides in concrete has been employed. The NDT method has been proved in conventional concretes (Figure 43).

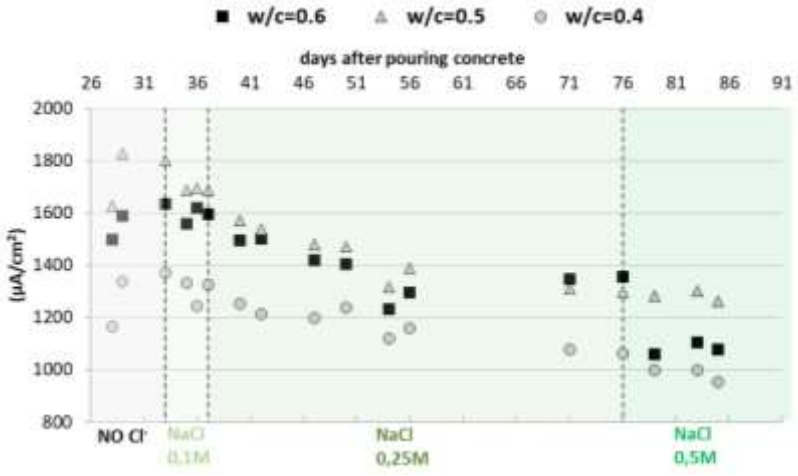

Figure 43. Results of parameter Cl^- for silver voltammetric sensors embedded in concrete w/c=0.6, w/c=0.5 and w/c=0.4. The different concentrations of chlorides (0.1M, 0.25M and 0.5M) refer to the solutions in which the concrete specimens were submerged.

In these sensors, the technique of cyclic voltammetry is applied with a three electrodes system, obtaining a response in intensity. When this response is processed the parameter Cl^- is obtained, which allows identifying variations in the amount of chlorides present in the cementitious matrix as shown in Figure 43.

Currently, these sensors have been embedded in XS1 and XS2 concretes, checking that there is a response, although, being the test still in progress, no conclusion can be drawn up.

3.3.2. Concrete pH evolution

The use of voltammetric sensors for pH measurement in hardened concrete matrices is under development, and data are still not sufficient to draw conclusions. In these sensors, the cyclic voltammetry technique is applied, obtaining an electric current response. This response is processed, obtaining the relevant parameter. A calibrated curve is needed to identify the pH changes of the concrete.

These sensors are well-calibrated in well known alkaline pH-solutions. The method is currently being tested in conventional concrete (CC and HPC) and ultra-high performance concrete (XS1 and XS2) matrices.

The first results at the early ages of the concretes show a coefficient of variation (CV) lower than 4% in all cases, with respect to the pH measured by the in situ leaching method (ISL) described by [Sagües et al., 1997]. Table 5 shows the pHs estimated by the sensor for each concrete at a specific age.

Table 5. Results of pH obtained by a voltammetric sensor.

Concrete	Days from mixing	pH measured by in situ leaching method	pH estimated with the sensor
XS1	36	13.2	12.8
CS2	31	12.9	13.1
CC	24	12.9	12.9
HPC	19	12.6	12.4

3.4. Corrosion risk of reinforcement

3.4.1. Corrosion potential (E_{CORR})

The main factors that may affect the reliability of E_{CORR} measurement in UHDC were studied and, subsequently, E_{CORR} was measured according to the standard method UNE 112083. The analyzed factors were the following:

- Distance between the reference electrode and the reinforcing bar
- Validity of the commercial reference electrodes
- Long-term stability of reference electrodes embedded in concrete
- E_{CORR} differences between the embedded and external reference electrodes
- E_{CORR} monitoring in NaCl immersion conditions to detect corrosion onset

a) <u>Distance between the reference electrode and the rebar. Validity of the commercial reference electrodes</u>

To perform the E_{CORR} test, it is appropriate that the reference electrode (RE) is located near the reinforcing bar to establish a reliable electrolytic connection between both (bar and RE). In the case of UHDC, its high resistivity can make this connection difficult, affecting the reliability of the results.

To analyze the effects of the distance between the reference electrode and the reinforcing bar on the E_{CORR} in this type of concrete, two concrete prisms were manufactured (100x100x400 mm). Two 8 mm diameter steel bars were embedded in one of the ends, the first one un-oxidized and the other one slightly oxidized (Figure 44). E_{CORR} measurements were taken by placing the reference electrode at different distances from the bars: 10, 50, 100, 150, 200, 250, 300 and 350 mm.

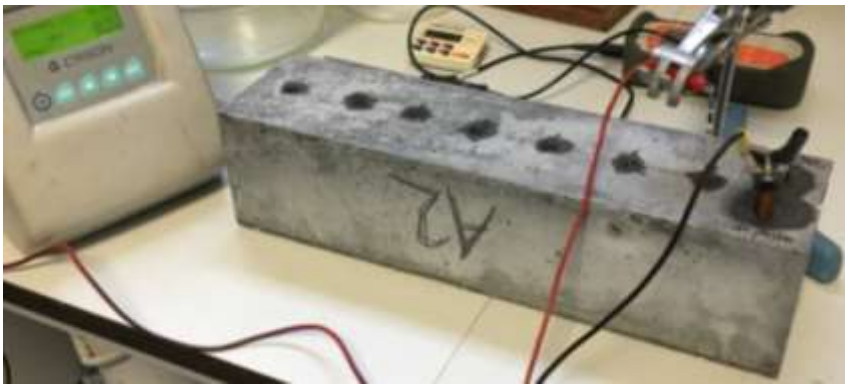

Figure 44. Corrosion potential set up varying the distance between the reference electrode and the rebar.

Moreover, in order to check the validity of the commercial reference electrodes that can be embedded in the concrete and which do not require maintenance, the study was carried out with two of them, a Mn/MnO_2 one and a Ag/AgCl one. The measurements were also carried out with a calomel electrode, which acted as a reference but as a surface electrode. The use of embedded in concrete allows continuous monitoring of the E_{CORR}.

Figure 45 shows the corrosion potential measurements in terms of the distance between the reference electrodes and the reinforcing bar. In the particular case of the calomel electrode (SCE), which is a surface application laboratory standard reference electrode, the results obtained show that the values of E_{CORR} do not vary significantly with the distance, at least up to 350 mm distance, so it is feasible and reliable to measure this parameter in the UHDC within the range of distances analyzed.

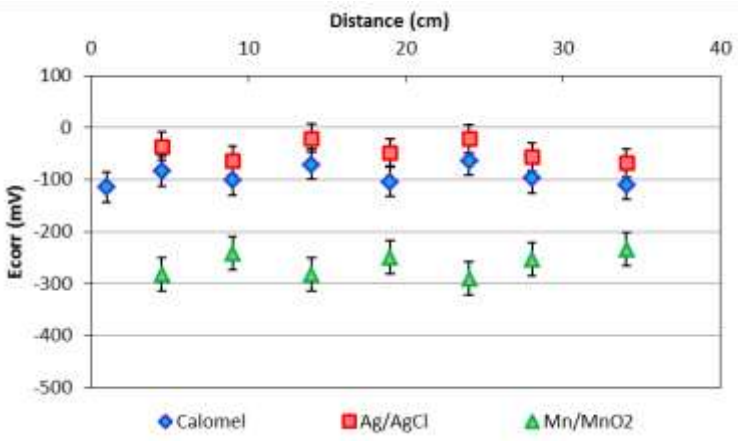

Figure 45. E_{CORR} as a function of the distance between the reference and the rebar.

As regards the reliability and sensitivity of Mn/MnO_2 and Ag/AgCl commercial reference electrodes embedded in concrete, the E_{CORR} values recorded have also not undergone significant variations depending on the distance, the differences between the commercial ones and the SCE holding constant. These differences have been on average -180mV for the Mn/MnO_2 electrode and +45 mV for the Ag/AgCl. These potential differences in relation to SCE practically coincide with the calibration performed before the start of the test, which was -184 mV vs SCE in the Mn/MnO_2 and +47 mV vs SCE in the Ag/AgCl electrode. That is, a constant ratio of conversion potentials is maintained between the different reference electrodes.

In conclusion, in UHDC it is possible to measure the E_{CORR} in situ with any of the three reference electrodes analyzed, all presenting a similar reproducibility.

b) <u>Long-term stability of reference electrodes embedded in concrete</u>

The long-term stability of the commercial reference electrodes that can be embedded in the concrete has been tested on an Mn/MnO_2 electrode. For this purpose, 100 mm cubic specimens were used and the reference electrodes were introduced near the surface. Before introducing the electrodes their potential vs SCE was measured. The specimens have been kept in the laboratory atmosphere. The monitoring has been carried out for almost a year in four types of concrete: CC, HPC, XS1 and XS2.

As shown in Figure 46, the electrodes embedded in the four concretes have a significant variation of the potential compared to the initial values. After 350 days, the potential is, on average, 160 mV more negative and it is not observed that the values tend to stabilize.

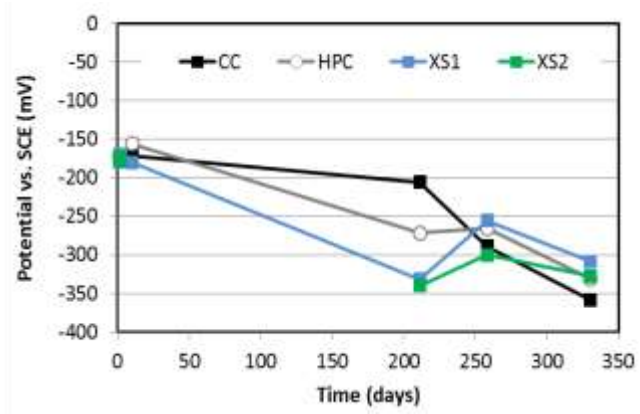

Figure 46. Long-term stability of a Mn/MnO_2 reference electrode embedded in concrete and kept in the laboratory atmosphere.

c) <u>Ecorr differences between the embedded and external reference electrodes</u>

The comparison of the E_{CORR} values obtained on the reinforcing bars of 2 specimens of CC, HPC, XS2, and XS2-CA+CN concretes with the external and the embedded (EMB) reference electrodes shows different behaviors depending on the environmental conditions (Figure 47). In the environment with 20ºC and 100% RH, the values of E_{CORR} obtained through both reference electrodes show that they are proportional and not very different independently of the type of concrete. However, two different evolutions of the potential between both measurements are detected in the specimens cured at 50% RH and 20ºC. The measurements of E_{CORR} for the XS2 and XS2-CA+CN concretes coincide, while those for the HPC and CC concretes diverge. The latter are drier in this condition due to their higher porosity and

loss of moisture. The moistures inside and on the surface of the concrete are different and that is why there are more differences between measuring with the embedded or external electrode. When the specimens are immersed in the NaCl solution the difference of E_{CORR} measured with the external and embedded reference electrodes is proportional and small due to the saturation of the specimens.

The use of embedded or external reference electrodes for E_{CORR} measurements can indicate differences with the type of concrete according to the environmental conditions employed.

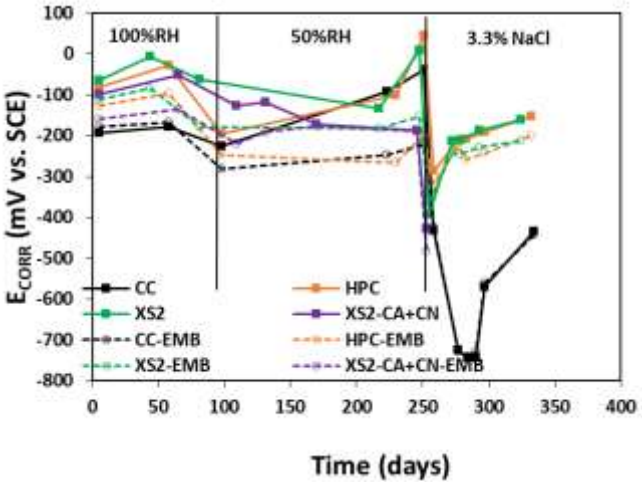

Figure 47. Comparison of E_{CORR} obtained with the external and embedded (S) reference electrodes over curing time (50% RH and 20ºC): left) CC and HPC; right) XS2 and XS2-CA+CN.

d) E_{CORR} monitoring to detect corrosion onset

Cubic test specimens (150x150x150 mm) with an embedded bar were manufactured for the test. After curing (60 days in a chamber at 20ºC and 100% RH), the specimens were cut to get a concrete cover thickness of the bar of about 10 mm and were placed in two different environments: 1) a room with 50% RH and 20ºC, employed by CSIC, and 2) submerged in a 3.3 wt% NaCl solution, employed by UPV and CSIC. The measurements were performed periodically and continuously.

The tests carried out in submerged specimens were performed following the recommendations of the method proposed by Tang et al. [2018]. All concrete surfaces of each specimen were coated with epoxy resin, except the surface to be exposed to the NaCl solution (Figure 48). This was done in order to ensure a unidirectional ingress of chlorides during the exposure period and to avoid oxidation of the rebar in the protruding zone.

In addition, CSIC subjected the XS2 specimens to several drying levels, varying the temperature and the exposure time, to reach different depth levels of the penetration of chlorides. Four specimens were exposed for 4 weeks at 50°C, three specimens one week at 100 °C and one specimen two weeks at 100 °C. Another two specimens, those have an embedded commercial electrode (Mn/MnO), 250 days at 20ºC and 50% RH. This pre-drying procedures were also applied to HPC and CC concretes with higher w/b ratio and porosity, managing to reach the surface of the rebar and initiating the corrosion, to be detected by the variations produced in the E_{CORR}.

Figure 48. Specimens used to measure E_{CORR}.

In the specimens kept in an environment at 50% RH and 20ºC, the evolution of corrosion potential vs. SCE of the reinforcing bars of the specimens of the different concretes (CC, HPC, XS2, and XS2-CA+CN) is shown in Figure 49. The average measured initial values for XS2 and XS2-CA+CN are very similar and vary between -105 and +114 mV vs. SCE in these environmental conditions. The presence of nanoadditions does not seem to exert a clear modification in the corrosion potential. With the curing time, the E_{CORR} of these four concretes is shifting to more positive potentials, becoming nobler. The values indicate the permanence of passive state and no corrosion initiation is detected.

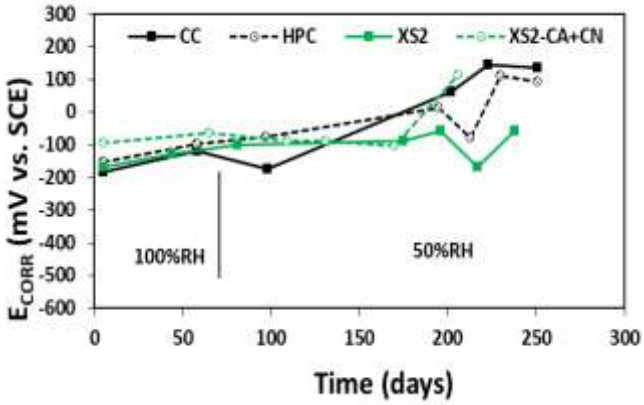

Figure 49. E_{CORR} at different ages for CC, HPC, XS2, and XS2-CA+CN concretes.

According to ASTM C876 or UNE 112083 standards, summarized in figure 16, E_{CORR} values below -200 mV vs. SCE indicate that there is a moderate probability that the rebars are corroding. Therefore, in the specimens where the E_{CORR} is more positive, the rebar is in the passivity region.

The CC and HPC concretes show E_{CORR} values quite similar to those obtained for the reference and with additions UHDCs, as well as an evolution of potential corrosion over time towards more positive values. Average E_{CORR} values measured for CC and HPC vary between -174 and +145 mV vs. SCE at 50% RH and 20ºC. These values confirm that the steel is found in a passive state in all studied concretes.

As regards the specimens submerged in a 3.3 wt% NaCl solution, Figure 51 shows the evolution of the corrosion potential vs. SCE of the rebars of a specimen of one of the studied concretes (XS1 concrete). During the first weeks of the test, unexpected large potential steps were recorded, which were distorting the measurements. These steps could possibly be motivated by the oxidation of the steel fibers on the surface, which after cutting the specimen remained exposed (Figure 50, left). This superficial oxide was cleaned with phosphoric acid 0.1 M (Figure 50, right). After this, the measurements were much more stable, so the cleaning procedure was repeated once a month.

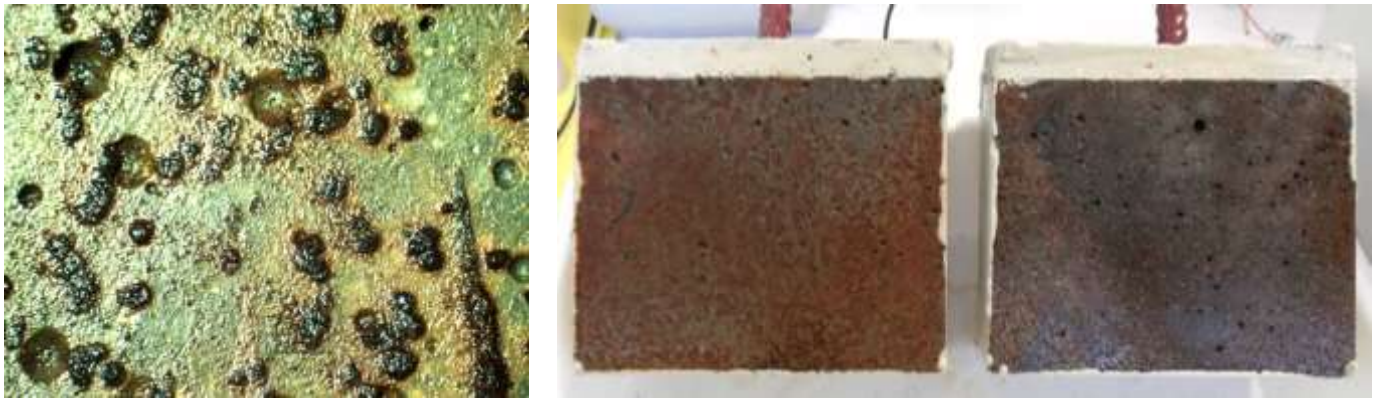

Figure 50. Oxidation of the surface steel fibers (left); specimens before and after the superficial phosphoric acid cleaning (right).

Independently of these abrupt potential changes, in Figure 51 it can be observed that the recorded values and their evolution over time are very similar to those obtained in the concrete XS2 kept at 20ºC and 50% RH (Figure 49), which indicates that the corrosion of the rebars has not occurred. During the first days, the E_{CORR} of several specimens is quite different (between -430 and -130 mV), although these values tend to slowly equalize to less negative values. For instance, at the age of 220 days, the E_{CORR} of all XS1 specimens (ten specimens) only varies between -15 and -130 mV.

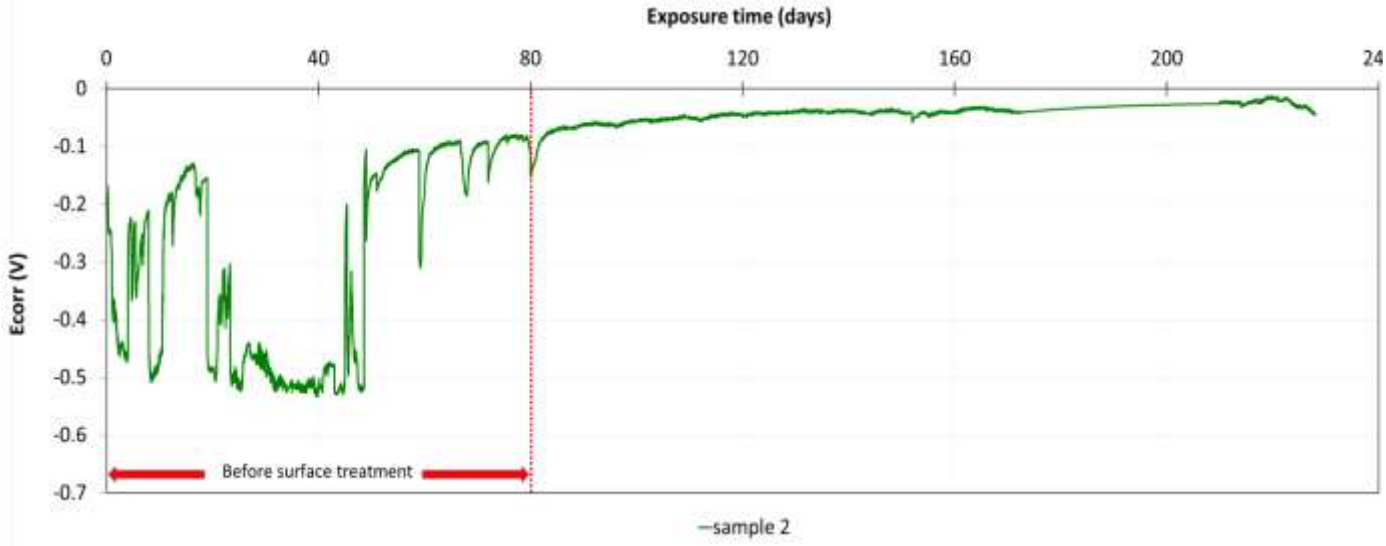

Figure 51. Evolution in time of E_{CORR} (XS1 concrete).

Figure 52 shows the evolution of the corrosion potential over time for the CC, HPC and XS2 specimens subjected to different pre-drying processes and immersed in a 3.3 wt% NaCl solution. During the first hours, the XS2 specimens present E_{CORR} values very negative, between -400 and -600 mV vs. SCE, but they increase progressively over time until they stabilize after 10 days in more noble values. From this moment, E_{CORR} values are found in the range of -240 and -155 mV vs. SCE, independently of the heat treatment, which indicates the breakdown of the passive film has not taken place by the presence of chloride ions and the steel stays in the passive state.

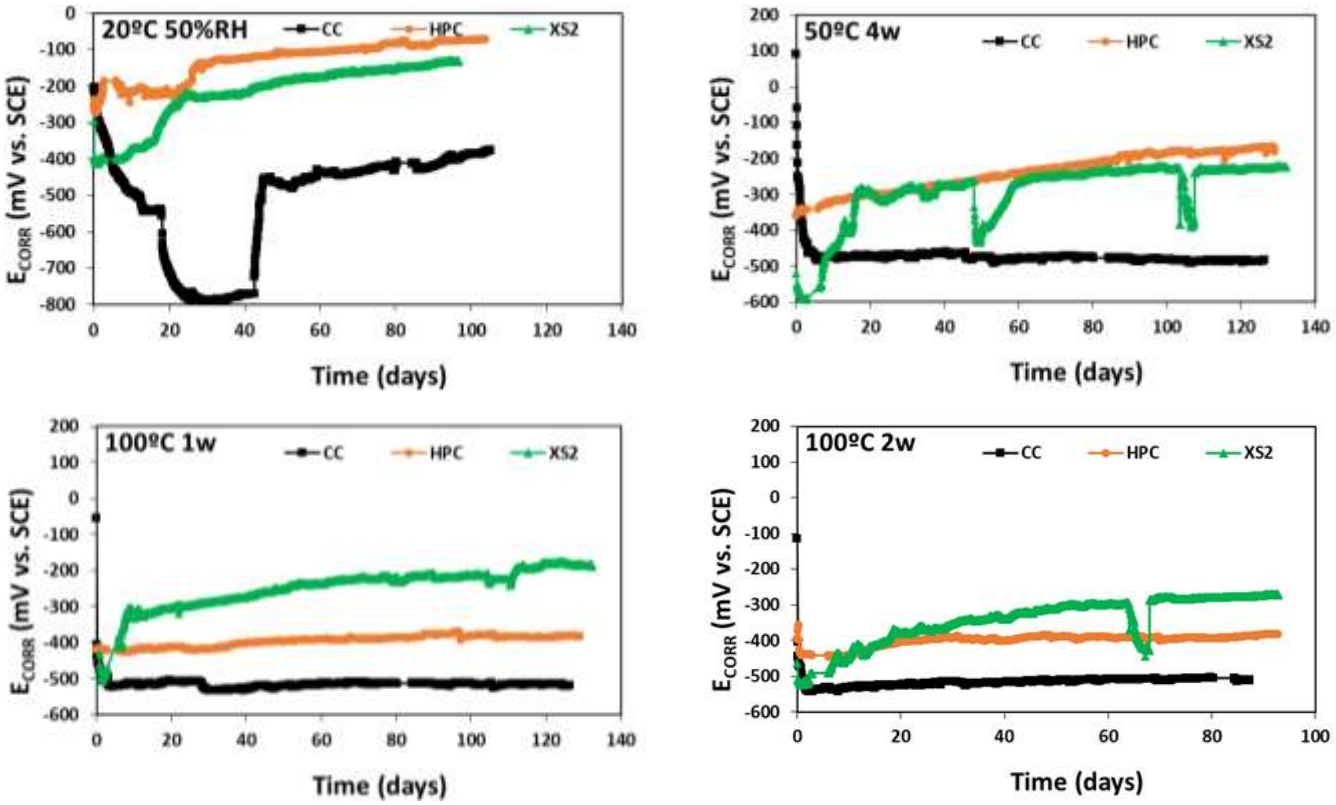

Figure 52. Evolution of E_{CORR} over time for CC, HPC and XS2 concretes exposed to different predrying level and immersed in NaCl solution.

In the case of HPC and CC concretes, clear variations can be observed in the E_{CORR} values according to the pre-drying treatment employed and the type of concrete. For HPC, it is more permeable than XS2 concrete and when the specimens are dried at 100ºC for 1 or 2 weeks, the chloride ions dissolved in water penetrate easily and the rebar corrosion onset takes place at early ages (E_{CORR} ≈ -400 mV vs. SCE). However, the specimens dried at 50ºC for 4 weeks or those exposed to natural drying, at 50% RH and 20ºC, show values of E_{CORR} between -100 and -225 mV vs. SCE, indicating the steel remain in a passive state.

For the CC, regardless of the predrying process, active E_{CORR} values are detected, around -500 mV vs. SCE from the beginning of the test. The specimens kept at 50% RH and 20ºC present initial E_{CORR} values around -180 mV vs. SCE. The potential decreases progressively and reaches values of -400 mV vs. SCE at 5 days of immersion. This value remains practically constant throughout the entire test, although there is a period of time where E_{CORR} values are more negative, probably due to the presence of oxygen and changes on the passive layer.

The main conclusion with respect E_{CORR} non-destructive technique is that it is valid for UHDC. For more accurate measurement the reference electrode should be placed near the reinforcing bar, obtaining reliable values with separations of up to 350 mm at least. Mn/MnO_2 and Ag/AgCl commercial reference electrodes present a similar reproducibility, although there may be significant differences in the results if the electrodes are embedded or surface located. Furthermore, it has been observed that the reference electrodes embedded in the concrete may not be stable in the long-term. It would be advisable to verify periodically their potential vs an outside calibrated electrode. This technique allows observing differences in the measurements carried out with the external or embedded reference electrodes according to the environmental conditions. In addition, the corrosion onset can be

detected at a certain time depending on the type of concrete and the ability of chloride entrance with this NDT technique.

It must also be taken into account that the oxidation of steel fibers on the surface may cause distortions in the values of E_{CORR}.

3.4.2. Corrosion rate (i_{CORR})

Firstly, some factors that may affect the reliability of i_{CORR} measurement in UHDC were studied by UPV and CSIC and subsequently corrosion rate was measured taking into account these aspects. The analyzed factors were the following:
- Influence of the separation between reinforcing bars and both the reference and auxiliary electrodes
- I_{CORR} differences between the embedded or external reference electrodes
- Corrosion rate measurement

a) Influence of the distance between rebars and both the reference and auxiliary electrodes on the reliability of the corrosion rate measurement in UHDC

For the measurement of the corrosion rate, it is advisable that both the reference and auxiliary or counter electrodes are placed as close as possible to the bar, in order to ensure an optimal electrolytic connection between them. In the specific case of UHDC, its high resistivity may hinder this connection affecting the reliability of the results.

To analyze how the distance between the reinforcing bar and either electrode in this type of concrete influence on the measurement of the i_{CORR} several prismatic XS1 concrete specimens were cast (100x100x400 mm). Two 8 mm diameter bars were embedded in one of the edges (Figure 53). A saturated calomel electrode (SCE) was used as reference electrode and a stainless-steel plate was used as auxiliary electrode. Measurements of the i_{CORR} were performed by placing the reference electrode at different distances: 50, 150, 250 and 350 mm. These measurements were performed as well with the auxiliary electrode at 2 distances: 30 and 370 mm.

Figure 53. Corrosion current density set up varying the distance between the reference electrode, the counter electrode, and the rebar.

Figure 54 shows the measurement of the corrosion current density as a function of the distance between the reference electrode and the reinforcing bar, for two different distances from the counter electrode (300 and 370 mm).

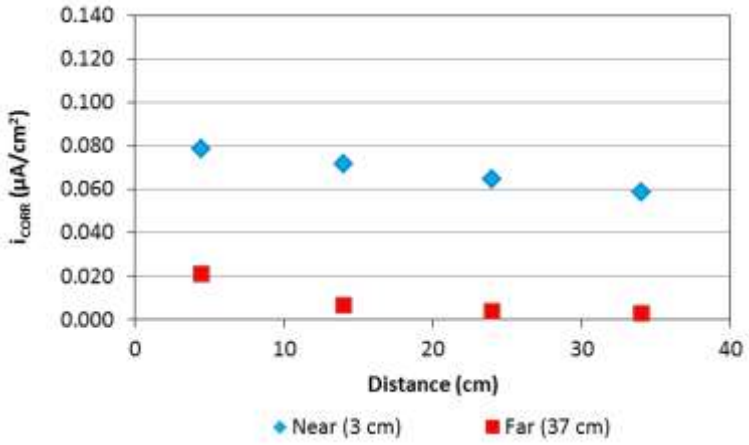

Figure 54. i_{CORR} as a function of the distance between the reference, the counter electrode and the rebar.

The results show that as the spacing between the reinforcement and the reference electrode increases, the current density values obtained are increasingly lower. For this reason, and to avoid wrong readings, the reference electrode should be placed as close as possible to the rebar in UHDC.

Likewise, it is observed that when the counter electrode is located away from the reinforcement, the i_{CORR} obtained is clearly smaller. That is why this electrode should also be placed near the rebar in UHDC.

b) I_{CORR} differences between the embedded or external reference electrodes

The comparison between the i_{CORR} values obtained measuring with external and embedded (Mn/MnO_2) electrodes were made in cubic specimens (15 cm), cured at 50% RH and 20ºC, the same ones that were employed in the corrosion potential measurements. Two E_{CORR} commercial sensors ($Mn/Mn\ O_2$) were embedded in two specimens of each type of concrete to know the reliability and sensitivity of the reference electrodes used to measure the corrosion current density.

Figure 55 shows the comparison of the corrosion current density i_{CORR} values measured of the rebars of two specimens of CC, HPC, XS2, and XS2-CA+CN concretes with the external and the embedded (EMB) reference electrodes according to the environmental conditions. The difference between the values obtained using the external or embedded reference electrodes are very small, practically coinciding and the trend over time is similar for the HPC, XS2, and XS2-CA+CN concretes independently of the exposure environmental. However, for CC these differences depend on the environmental conditions, specifically higher discrepancies of i_{CORR} are observed at 20ºC with 100% or 50% RH.

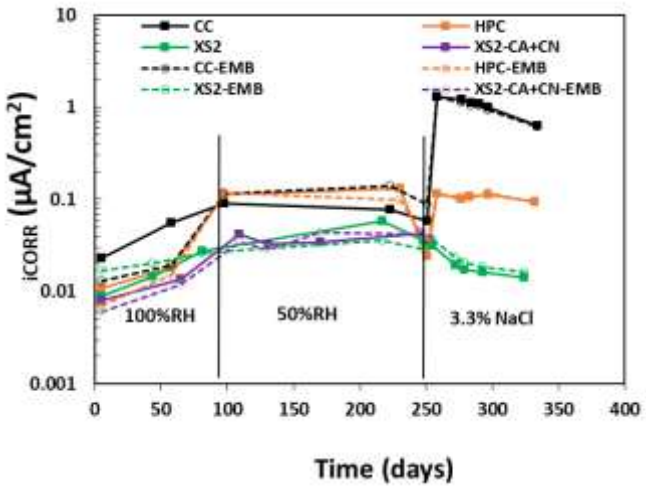

Figure 55. Comparison of i_{CORR} obtained with the external and embedded (EMB) reference electrodes over curing time in CC, HPC, XS2, and XS2-CA+CN concretes exposed to different environmental conditions.

c) Corrosion rate monitoring

The corrosion current density (i_{CORR}) in the reinforcing bars embedded in the different concretes was measured according to the standard method UNE 112072 by CSIC using linear polarization method (with an AUTOLAB 84750 potentiostat /galvanostat) and according to Tafel method by UPV (using an AUTOLAB PGSTAT10 potentiostat/galvanostat). This parameter was monitored in the same 10 specimens used for the corrosion potential determination, employing the same three-electrode cell configuration. As described in section 3.4.1.d, the concrete cover of the bar is 10 mm and the specimens were placed in two different environments: 1) a room at 50% RH and 20ºC, employed by CSIC, and 2) submerged in a 3.3 wt% NaCl solution, employed by UPV and CSIC. CSIC also subjected the specimens to different pre-drying treatments.

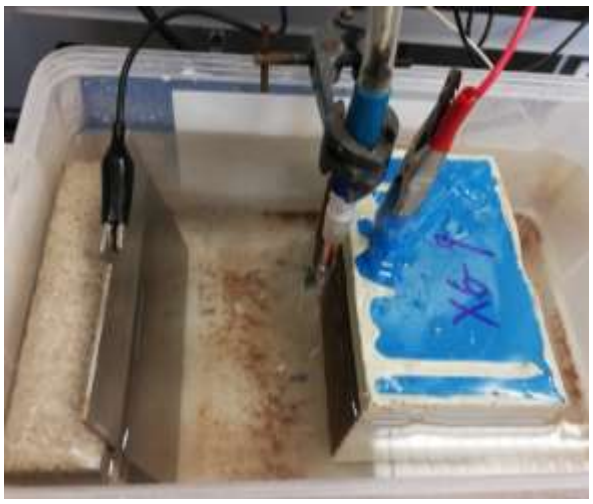

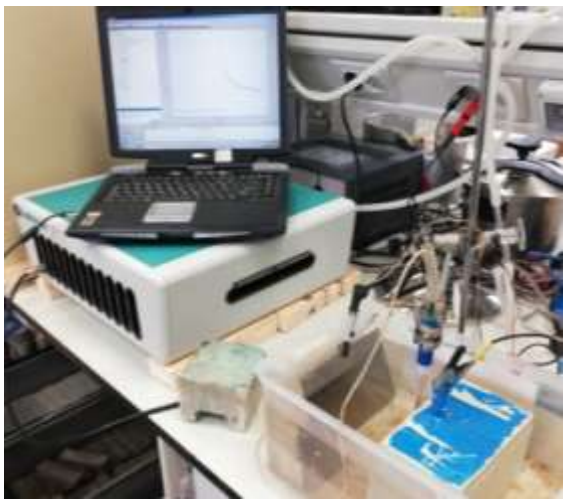

Figure 56. Test of corrosion rate.

In the specimens kept in an environment at 50% RH and 20ºC, the evolution of i_{CORR} of the rebar of 10 specimens of each studied concrete designed for XS-Mediterranean offshore environment is shown in Figure 57. The average initial i_{CORR} values for XS2 and XS2-CA+CN vary between 0.035 and 0.090 µA/cm^2. These values are very low regardless of the

type of cement and nanoaddition incorporated, corresponding to negligible corrosion, which is below 0.1 µA/cm^2. The presence of nanoadditons does not imply differences in the measurement of i_{CORR} in a passive state.

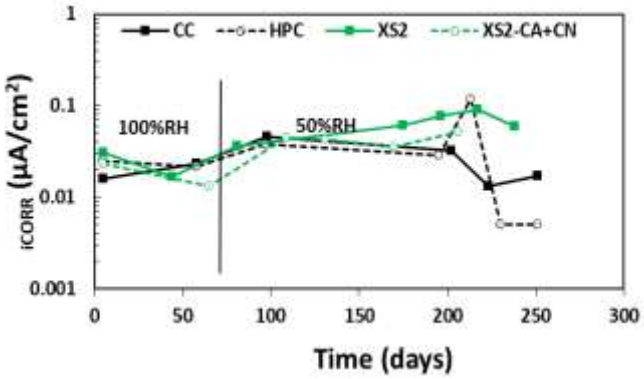

Figure 57. i_{CORR} at different ages for CC, HPC, XS2, and XS2-CA+CN concretes.

For the case of traditional concretes (CC and HPC), the average i_{CORR} values measured are in the range of 0.005 to 0.118 µA/cm^2 throughout 200 days. No differences in this parameter are observed with respect to the XS2 and XS2-CA+CN concretes.

As regards the specimens submerged in a 3.3 wt% NaCl solution, Figure 58 shows the evolution of the average corrosion density (i_{CORR}) of the reinforcing bars in the 10 specimens of XS1 and XS1-CA+ANF concretes. As can be seen, the values of i_{CORR} after 200 days of exposure to chlorides are very low, between 0.01 and 0.02 µA/cm^2, and therefore clearly within what is related to as negligible corrosion, which is below 0.1 µA/cm^2. These results are very similar to those obtained in the specimens kept at 20ºC and 50% RH (Figure 57) and are consistent with the E_{CORR} values recorded.

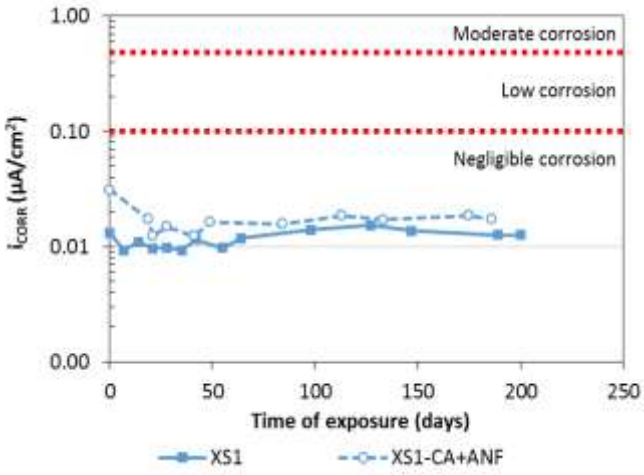

Figure 58. Evolution of i_{CORR} of specimens exposed to chlorides.

Figure 59 shows the evolution of the corrosion current density over time for the CC, HPC and XS2 specimens subjected to different levels of pore drying and immersed in a 3.3 wt% NaCl solution. Throughout the test, the XS2 concretes present i_{CORR} values below 0.1 µA/cm^2 regardless of the pre-drying level. Therefore, it is clear that although if the drying is very intense, the bars embedded in the UHDCs do not detect corrosion onset.

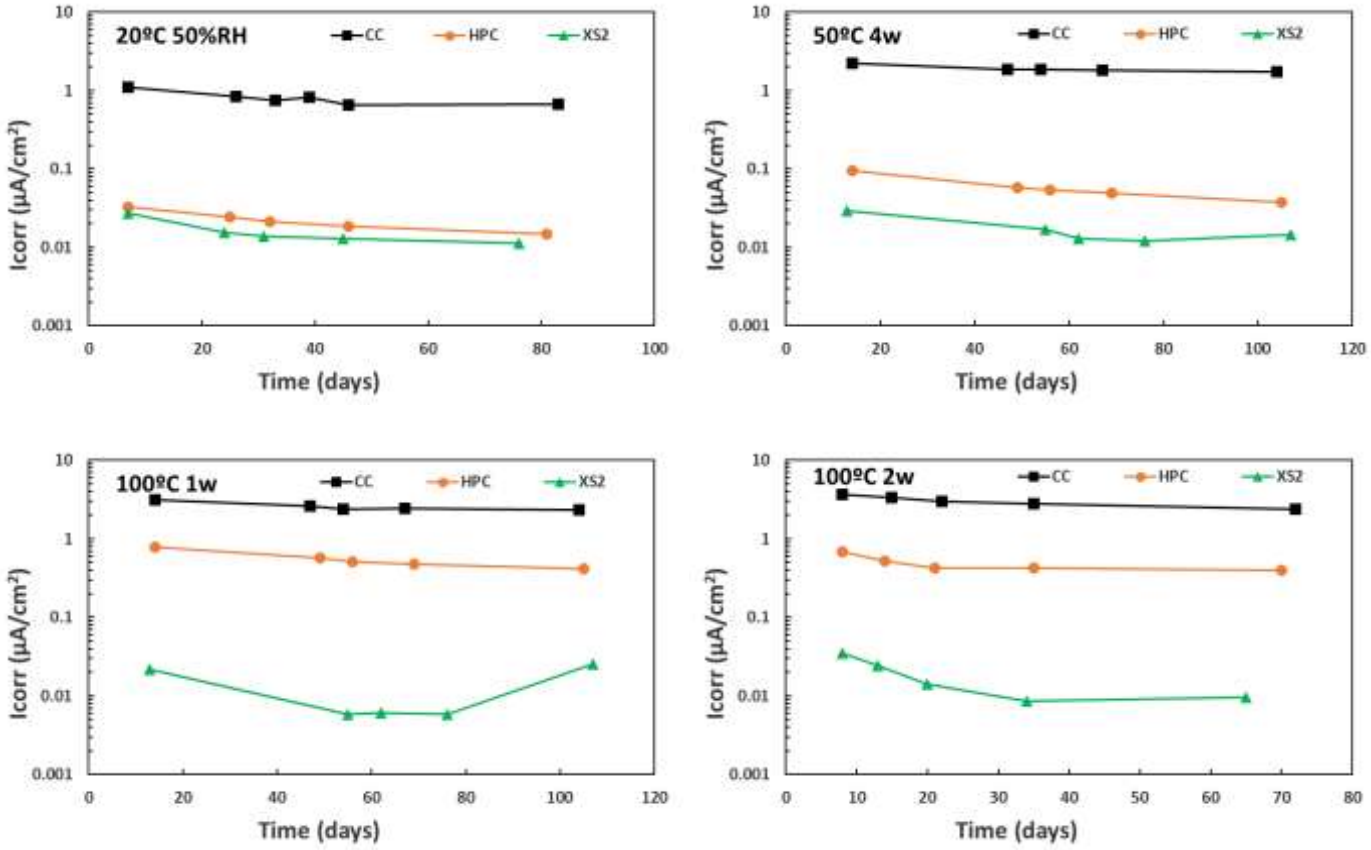

Figure 59. Evolution of i_{CORR} over time for CC, HPC and XS2 concretes exposed to different pre-drying levels and immersed in NaCl solution.

However, the pore drying level greatly influences on the value of i_{CORR} developed by the bars in the HPC and CC concretes. A lower level of pore drying to the HPC specimens, 50ºC for 4 weeks or an exposition at 20ºC and 50% RH, are not enough for chloride ions to reach the rebar and to breakdown the passive layer and i_{CORR} values below 0.1 µA/cm^2 are observed.

Nevertheless, the intense pre-drying applied in HPC, or the three pre-drying levels and the exposition at 20ºC and 50% RH in CC, are weak enough to facilitate the penetration of chloride aggressive ions for the reinforcing bars and initiate corrosion, detecting high values of i_{CORR}. A high corrosion risk is observed for the CC specimens pre-dried at 50ºC for 4 weeks, 100ºC for 1 or 2 weeks, while the CC specimens that kept drying at room temperature and the HPC specimens dried at 100ºC for 1 or 2 weeks show corrosion onset and a moderate corrosion level.

The main conclusion is that i_{CORR} non-destructive technique is suitable for use with UHDC. The reference electrode and the counter electrode should be placed near the rebar to avoid wrong readings. No differences have been observed in the i_{CORR} measurements for UHDCs carry out with the external or embedded reference electrodes according to the environmental conditions. Moreover, the corrosion onset can be detected at a certain time depending on the drying level of pores and the penetration of Cl and the type of concrete.

4. Recommendations

The sensitivity and reliability of non-destructive methods commonly used in conventional concretes had to be evaluated in UHDCs due to the high content of fibres and the high compactness of the matrix. In order to serve as a basis to decide which are the most suitable techniques for in-situ measurements to be employed in large scale-up, at pilot-scale validation, the analysis is summarized below and the most relevant conclusions are compiled in Table 6.

Durability indicators related to mechanical parameters:

- Ultra-pulse velocity technique has limited sensitivity with ultra-high-density concretes differences and with the ageing, being all the values obtained with UHDC very similar. However, this technique can be used to detect crack damages. Both direct and indirect methods have demonstrated sensitivity.
- The acoustic emission test is an effective test in UHDC and shows good reliability and sensitivity in cracked concrete. It can be used to detect the crack damages of structures made with UHDC and monitoring their health (first cracks could be detected).
- Strain gauges can be used to measure deformations. The measurements can be performed in a continuous mode and remotely. In high humidity environments a multi-layer protection of the strain gauge is essential.

Durability indicators related to physical parameters:

- Gas Permeability NDT method is valid for UHDC, even in cracked state, and therefore it can be used to characterize these concretes. For cracked state, UHDC values are close to a conventional concrete in uncracked state.
- The electrical resistivity shows a great sensitivity regarding the type of concrete and the presence of additions, and therefore it can be used to characterize UHDCs. However, due to the large discrepancies observed in the results when using specimens of different shapes and sizes, it is necessary to create a specific test protocol for this type of concretes. The direct method is less sensitive to detect cracks in UHDC concretes with high steel fibre content, while using indirect method (Wenner method) differences are well detected between cracked and uncracked concrete.

Durability indicators related to physical parameters:

- Changes in chloride activity in conventional concretes can be identified. Tests with UHDC are in progress.
- pH can be estimated with sensors and the error was less than 0.4 units.

Durability indicators related to corrosion risk of reinforcement:

- The E_{CORR} technique is valid for UHDC. The reference electrode should be placed near the bar to be monitored. The reference electrodes embedded in the concrete may not be stable in the long term. It would be advisable to verify periodically their potential vs. an outside calibrated electrode. The corrosion onset can be detected depending on the drying of concrete pores and the ability of chloride entrance and the type of concrete. It must also be considered that the oxidation of steel fibres on the surface may cause distortions in the values of E_{CORR}. Likewise, the absence of oxygen entails more negative E_{CORR} values than in more porous concretes.
- The corrosion rate determination is suitable for using with UHDC. The LPR and the Tafel method can be considered acceptable for monitoring the evolution of the corrosion processes and detection of corrosion onset. The reference electrode and the counter electrode must be placed near the rebar. No differences have been observed in the i_{CORR} measurements for UHDCs carry out with the external or embedded reference electrodes according to the environmental conditions.

Table 6. Main features of NDT methods for use with UHDCs.

Concrete	**Mechanical parameters**	**Ultrasonic pulse velocity**	- Low sensitivity to distinguish between UHDCs of different compositions - Low sensitivity to distinguish between UHDCs of different ages - High sensitivity to detect crack. Both direct and indirect methods are valid.	External implementation
		Acoustic emission	- Valid method to detect cracks and the extent of damages	External implementation
		Deformation	- Strain gauges can be used to measure concrete surface deformation.	External implementation (*)
	Physical parameters	**Gas permeability**	- Valid method to characterize UHDCs - Valid method for UHDC even in cracked state	External implementation
		Electrical resistivity	- Valid method to characterize UHDCs - Low sensitivity of the direct method to detect cracks - The Wenner method is selective to crack detection	External implementation
	Chemical parameter	**pH**	- Sensors can be used to estimate the pH value of UHDC	Embedded implementation
Reinforcement	**Corrosion risk**	**Corrosion potential**	- Valid method to detect the rebar corrosion onset - The reference electrodes embedded in the concrete may not be stable in the long-term - Oxidation of surface steel fibres may cause distortions in the E_{CORR} measurement - The moisture content influences in E_{CORR} measurement. High moisture gives good correlation between embedded and surface reference electrodes	External / Embedded implementation (*)
		Corrosion rate	- Valid method to detect the corrosion onset - Valid method to monitor the evolution of the corrosion process	External / Embedded implementation (*)

(*) Possibility of continuous and remote monitoring

The most remarkable output is that there are several options for selecting NDT techniques in all the scenarios. These parameters will provide suitable information to evaluate the durability of the UHDCs in scaling-up to the pilots.

Some NDTs can be implemented with automatic systems and data loggers for continuous monitoring and provide information in real-time, but in the embedded local positions. With surface sensors periodical data are collected distributed in different places of the structure.

5. References

- EN 12504-4 (2006). Testing concrete. Part 4: Determination of ultrasonic pulse velocity.
- GWT. (2014). *GWT.* Retrieved from http://germann.org/wp-content/uploads/2014/05/GWT.pdf
- Haindl K., Schörner T., Zirkelbach D., Fitz C (2016). Was ist bei Karsten & Co. zu beachten?, Bautenschutz + Bausanierung. Volume 39, issue 3, pages 33-37 , ISSN: 2190-9504, ISSN: 0170-9267 (in German). Permalink to online repository of German's "Fraunhofer-Gesellschaft": http://publica.fraunhofer.de/documents/N-399589.html. Free download (Oct. 28th, 2019) from https://wufi.de/literatur/Haindl, Schöner et al. 2016 - Was ist bei Karsten.pdf
- Ohno K., Ohtsu M. (2010). Crack classification in concrete based on acoustic emission. Constr. Build. Mater. 24: 2339–2346. doi:10.1016/j.conbuildmat.2010.05.004.
- Sagües A.A., Moreno E.I., Andrade C. (1997). Evolution of pH in-situ leaching in small concrete cavities. Cement and Concrete research, 27(11): 1747-1759.
- Scerivini M. (2009). Themoelectric Materials for Thermocouples. Retrieved April 11, 2019, from University of Cambridge, Department of Materials Science and Metallurgy: https://www.msm.cam.ac.uk/utc/thermocouple/pages/ThermocouplesOperatingPrinciples.html
- SIA, Swiss Standard 262/1 (2013). Concrete construction. Complementary specifications.
- Tang L., Frederiksen J.M., Angst U.M., Polder R., Alonso M.C., Elsener B., Hooton R.D., Pacheco J. (2018). Experiences from RILEM TC 235-CTC in recommending a test method for chloride threshold values in concrete. RILEM Technical Letters, 3: 25-31 DOI: http://dx.doi.org/10.21809/rilemtechlett.2018.55
- The Concrete Society. (n.d.). *Figg Test*. Retrieved from Concrete @ your Fingertips: http://www.concrete.org.uk/fingertips-nuggets.asp?cmd=display&id=572#
- UNE 83988-1 (2008). Concrete durability. Test methods. Determination of the electrical resistivity. Part 1: Direct test (reference method).
- UNE 112083 (2010). Measurement of free corrosion potential on steel reinforced concrete structures.
- UNE 112072 (2011). Laboratory measurement of corrosion speed using the polarization resistance technique.